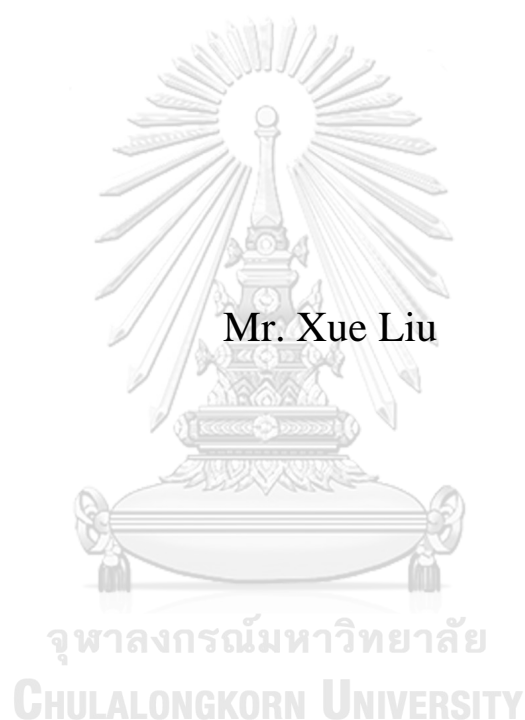


Rice granules as natural carrier to encapsulate drug and aromatic oils



A Dissertation Submitted in Partial Fulfillment of the Requirements
for the Degree of Doctor of Philosophy in Nanoscience and Technology
Inter-Department of Nanoscience and Technology
GRADUATE SCHOOL
Chulalongkorn University
Academic Year 2019
Copyright of Chulalongkorn University

กรานูลข้าวจากธรรมชาติสำหรับเป็นโมโนลิธคดีพอทเพื่อประยุกต์นำส่งยา



วิทยานิพนธ์นี้เป็นส่วนหนึ่งของการศึกษาตามหลักสูตรปริญญาวิทยาศาสตรดุษฎีบัณฑิต
สาขาวิชาวิทยาศาสตร์นาโนและเทคโนโลยี สหสาขาวิชาวิทยาศาสตร์นาโนและเทคโนโลยี

บัณฑิตวิทยาลัย จุฬาลงกรณ์มหาวิทยาลัย

ปีการศึกษา 2562

ลิขสิทธิ์ของจุฬาลงกรณ์มหาวิทยาลัย

Thesis Title	Rice granules as natural carrier to encapsulate drug and aromatic oils
By	Mr. Xue Liu
Field of Study	Nanoscience and Technology
Thesis Advisor	Professor Supason Wanichwecharungruang, Ph.D.
Thesis Co Advisor	Associate Professor WIJIT BANLUNARA, D.V.M., Ph.D.

Accepted by the GRADUATE SCHOOL, Chulalongkorn University in
Partial Fulfillment of the Requirement for the Doctor of Philosophy

..... Dean of the GRADUATE
SCHOOL
(Associate Professor THUMNOON NHUJAK, Ph.D.)

DISSERTATION COMMITTEE

..... Chairman
(Associate Professor VUDHICHAI PARASUK, Ph.D.)

..... Thesis Advisor
(Professor Supason Wanichwecharungruang, Ph.D.)
..... Thesis Co-Advisor

(Associate Professor WIJIT BANLUNARA, D.V.M.,
Ph.D.)

..... Examiner

(Assistant Professor RATTHAPOL RANGKUPAN,
Ph.D.)

..... Examiner

(Assistant Professor SUKKANESTE TUNGASMITA,
Ph.D.)

..... External Examiner

(Associate Professor Sumate Ampawong, Ph.D.)

ชู หลิว : กราณูลข้าวจากธรรมชาติสำหรับเป็นโมโนลิธิคดีพอทเพื่อประยุกต์นำส่งยา. (Rice granules as natural carrier to encapsulate drug and aromatic oils) อ.ที่ปรึกษาหลัก : ศ. ดร.ศุภศร วนิชเวชรุ่งเรือง, อ.ที่ปรึกษาร่วม : รศ. นสพ. ดร.วิจิตร บรรณนารา

กราณูลข้าวจากธรรมชาติ คือ แหล่งพลังงานหลักของประชากรโลก มีการนำกราณูลข้าวไปใช้ประโยชน์อย่างแพร่หลาย เช่น ใช้เป็นอาหาร ยารักษาโรค รวมถึง อุตสาหกรรมสิ่งพิมพ์ และ พลาสติก ในงานวิจัยนี้ได้นำกราณูลข้าวจากธรรมชาติมาใช้ในการกักเก็บ และ นำส่งยาที่ละลายน้ำได้ คือ แวนโคไมซิน (Vancomycin) ได้ศึกษาการปลดปล่อยยาที่ถูกกักเก็บในตัวนำส่งนี้ทั้งในสภาวะที่เป็นกรด สภาวะที่เป็นด่าง สภาวะที่อุณหภูมิสูง รวมถึงสภาวะที่มีการย่อยอาหารด้วยน้ำย่อย ได้แก่ อะไมเลส (amylase) ทริปซิน (trypsin) และ ลิเปส (lipase) กราณูลข้าว 100% จากธรรมชาตินี้เป็นแคปซูลของเมทริกซ์ แบบไร้แกนและเปลือก (non-core-shell structure) ในที่นี้สามารถยืนยันการกักเก็บยาได้สำเร็จในกราณูลข้าว โดยการศึกษาความเป็นผลึก สมบัติทางความร้อน และหมู่ฟังก์ชันของกราณูลที่ถูกกักเก็บยาด้วยเทคนิค XRD TGA และ IR ตามลำดับ ผลการศึกษาการปลดปล่อยยาจากกราณูลข้าวพบว่า สามารถปลดปล่อยยาออกจากกราณูลได้ 70% จากปริมาณยาทั้งหมดที่ถูกกักเก็บ และ อีก 30% ยังถูกกักเก็บอยู่ในกราณูลเนื่องจากมีอันตรกิริยาที่แข็งแกร่งระหว่างยาและเมทริกซ์ของกราณูลข้าว นอกจากนี้ได้มีการกักเก็บน้ำมันหอมระเหย และศึกษาการกักเก็บและปลดปล่อยน้ำมันหอมระเหยจากกราณูลข้าว จากการประเมินผลโดยผู้เชี่ยวชาญพบว่า หลังจากเก็บอาหารจานที่มีส่วนผสมของกราณูลข้าวที่กักเก็บน้ำมันหอม เป็นเวลา 5 วัน แล้วอุ่นร้อนด้วยเตาไมโครเวฟ ยังมีกลิ่นหอมของน้ำมันหอมระเหยอยู่ กระบวนการในการกักเก็บนี้สามารถอธิบายได้ด้วย แบบจำลองทางคณิตศาสตร์ (mathematical model)

จุฬาลงกรณ์มหาวิทยาลัย
CHULALONGKORN UNIVERSITY

สาขาวิชา วิทยาศาสตร์นาโนและเทคโนโลยี
ปีการศึกษา 2562

ลายมือชื่อ นิสิต
ลายมือชื่อ อ.ที่ปรึกษาหลัก
ลายมือชื่อ อ.ที่ปรึกษาร่วม

5687839620 : MAJOR NANOSCIENCE AND TECHNOLOGY

KEYWORD starch encapsulation, vancomycin encapsulation, aromatic
D: encapsulation, rice granule

Xue Liu : Rice granules as natural carrier to encapsulate drug and aromatic oils. Advisor: Prof. Supason Wanichwecharungruang, Ph.D. Co-advisor: Assoc. Prof. WIJIT BANLUNARA, D.V.M., Ph.D.

Rice granules as major energy supply to humanity worldwide are utilized in many fields, such as food, medical, printing and plastic industries. In this thesis work, rice starch/granule is applied as hydrophilic drug (vancomycin) carrier to achieve the release. By confirmation on the stability of rice granules against to various treatments like alkali, acid and heating, as well as α -amylase, trypsin, and lipase, it is possible to use rice granules as 100% natural source to be the capsule and matrix getting the non-core-shell structure of the formation. The success of encapsulation is confirmed by the observations on crystalline, thermal properties and functional groups from XRD, TGA, and IR analysis. Release of vancomycin from rice granules was observed by experiments, but only 70% vancomycin encapsulated can be released out, another 30% is entrapped or combined with rice granule matrix very strong, leading the vancomycin kept inside starch matrix. In addition to aromatic oils encapsulations, the protective and released properties of rice granules are determined. The evaluation to the dishes with rice granules encapsulated with aromatic oils as seasonings by experts shows that dishes prepared by aromatic rice granules could achieve best results after 5 days storage when reheated by microwave-oven. A mathematical model is applied to explain the encapsulation process.



Field of Study: Nanoscience and
 Technology

Academic 2019
 Year:

Student's Signature

.....

Advisor's Signature

.....

Co-advisor's Signature

.....

ACKNOWLEDGEMENTS

The success of this thesis can be succeeded by the attentive support from Associate Professor Dr. Supason Wanichwecharungruang on kindly academic supervision during my progress of thesis work. Also, thanks to Associate Professor Dr. Wijit Banlunara for the experimental work in the Faculty of Medicine, and thanks to Assistant Professor Dr. Sumate Ampawong to the consultant works for the thesis.

Appreciate the committee and staff in Nano Science and Technology program, Graduate School and Chulalongkorn University for all the supports.

I would like to thank the entire respondent who was the sampling in this study.

Xue Liu

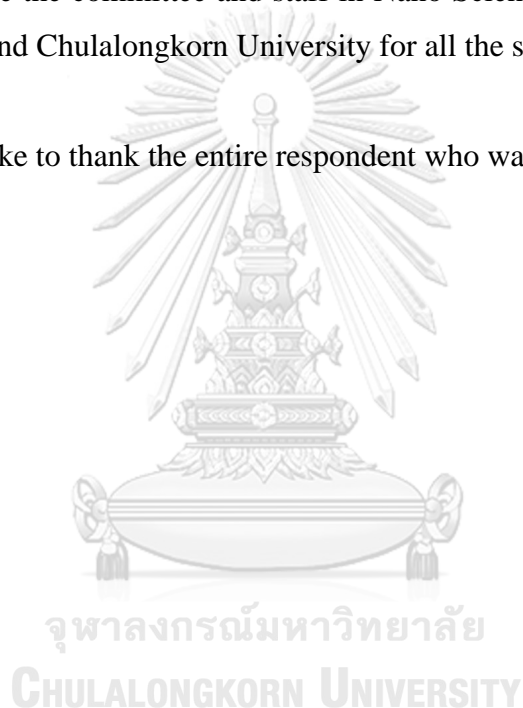


TABLE OF CONTENTS

	Page
ABSTRACT (THAI)	iii
ABSTRACT (ENGLISH).....	iv
ACKNOWLEDGEMENTS	v
TABLE OF CONTENTS.....	vi
Chapter I Literature review	9
1. Starch.....	9
1.1 Amylose.....	13
1.2 Amylopectin	17
1.3 Lipids and proteins	27
2. Vancomycin.....	32
3. Edible Oil encapsulation.....	34
Chapter II Materials and methods.....	38
1. Materials	38
1.1 Starch.....	38
1.2 Vancomycin.....	38
1.3 Curcumin.....	38
1.4 Enzymes	38
1.5 Edible aroma oils.....	39
2. Methods	41
2.1 Properties of rice granule in thermo-responsive swelling and shrinking .	41
2.2 Stability	42
2.3 Vancomycin encapsulation.....	43
2.4 Encapsulation of curcumin.....	44
2.5 Optimal microscopy	44
2.6 Vancomycin release from granules	44

2.7 Thermal Gravimetric Analyses	45
2.8 X-ray diffraction analysis	45
2.9 Tissue interaction	46
2.10 Edible oils encapsulation.....	46
2.11 Stability of oil (GO, HBO and LO) test	47
2.12 Gas Chromatography Mass Spectrometry (GC-MS) analysis	47
2.13 Applications in ready meals/fast foods	48
2.14 Sensory Taste evaluations	48
Chapter III Experimental results	50
1. Thermo-responsive size change of the rice granules.....	50
2. Stability of rice starch.....	52
3. Encapsulation of vancomycin.....	55
4. Encapsulation of curcumin	57
5. Release profile of vancomycin-loaded granules.....	58
6. TGA results	59
7. XRD results	61
8. Tissue interaction.....	62
9. Edible oils encapsulation	62
10. GCMS results	63
11. AVONA statistical analysis.....	70
Chapter IV Discussion	73
1. Granules to be carriers	73
2. Mathematical description of heating/encapsulation process	74
1.1 Diffusion.....	75
1.2 Hygroscopic swelling	76
1.3 Heating/Encapsulation.....	79
Chapter V Conclusion.....	89
REFERENCES	91
VITA.....	96

Chapter I Literature review

1. Starch

Starch contributes main energy supports to all humanities all over the world and generated as carbohydrate reserves from green plants. In natural, green plants cells and some micro-organisms, assimilations of CO₂ and H₂O happen to become energy source: glucose. Usually this energy is kept in roots, tubers, fruits, leafs, kernels, trunks and seeds as two polymeric glucose formations: amylopectin and amylose. The most principal resources for humans are tubes, roots, as well as cereals. Starch is formed in the positions called amyloplasts as dispersed particles or granules with different morphologies in distinct plants, states from oval ogival or round to lenticular or flat. The biosynthesis of starch particle/granule is started from hilum, grows by apposition. Starch granules/particles are densely wrapped with semi-crystalline architectures with density at around 1.5 kg/m³. Due to the stability of semi-crystalline, starch granule usually is not soluble in cold water. Before the gelatinization happens, starch granule could absorb water to swell up by keeping shape consistent. And this swelling process is reversible upon drying. Granular starch can be easily separated by gravity sedimentation, filtration or centrifugation, and could be treated by sundry chemical, physical and enzymatic/biological modifications with subsequent cleaning or processing. The way of categorizing the structure of starch granule is to classify the one into nano, micro or macro level respectively. For the rice granule specifically, three structure can be complicatedly complex with above levels of the three (also named as molecular or fine structure), with dimensions ranging from 7 Å (glucose molecule) to 400 nm (growth ring thickness)¹. Its complexity is based on the various structural formations, involving the polymer chains; chain-length distribution of amylopectin and associated degrees of branching; alternating semi-crystalline and amorphous growth rings; relative proportion of amylopectin and amylose. Basically, amylose in starch is not strictly linear, such as rice granule. Amylose in rice consists of blending of linear and slightly branched molecules (2-4 chains) with degree of polymerization (DP) of 700-900 and 1100-1700 glucose units². Amylose percentage in rice starch varies from 0% to 33%, and some mutant ones with 35-40% are also known³. The glucose units in rice amylose is much smaller than the one in rice

amylopectin, which is mostly having DP between 5000-15000 glucose units with each molecule consisting of 220-700 chains². Generally, properties of starch granule are summarized with crystallinity, lamella, blocklet and granular rings, with the researches achieved by X-ray, SEM, TEM and AFM devices. As mentioned above, rice granules are semi-crystalline containing both amorphous and crystalline regions. When granules treated by acid (usually dilute sulfuric or hydrochloric acid), the amorphous regions can be removed and crystalline remained. So the crystallites are formed by amylopectin, every two chains inside could join into the double-helix with 6 glucose residues per turn of each pitch and a strand of 2.1 nm, the length of double-helices is at 4-6 nm⁴. X-ray analysis explained that that the double-helices crystallizes into either of two polymorphs called A- and B-types (Figure 1), and the cross-section of double helices is illustrated in Figure 2⁵.

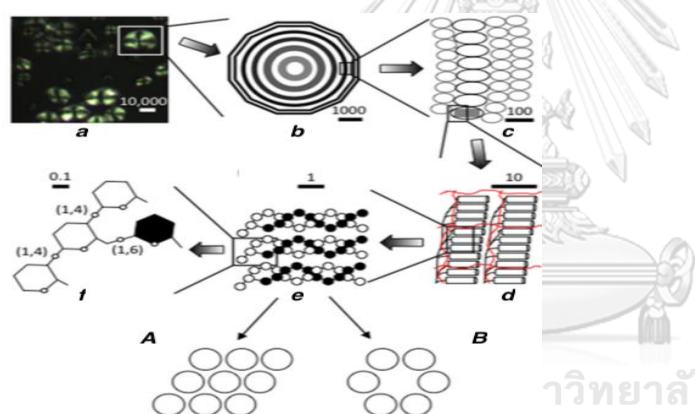


Figure 1. Dimensional information of starch granule: from granular level to glucosyl units: a. “Maltese cross” phenomenon under polar light observed from maize starch; b. Polyhedral hypothetical granule with growth rings expanding from hilum; c. Blocks in amorphous (grey and small) and semi-crystal (black and big) rings; d. Segments of amylopectin (black lines) and amorphous and crystalline lamellae formed by double helices branched (cylinders). Amylose (red lines) inter-distribute through amylopectin; e. Three double helices of amylopectin, each one contains two polyglucosyl chains, whereas glucosyl residues are represented by black and white circles. The double helices here are from A- and B- polymorphic crystals; f. Glucosyl units showing connections at α -(1,4) and α -(1,6) linkages in double helix. Bar scale is in nano meter to approximately indicate the situations.

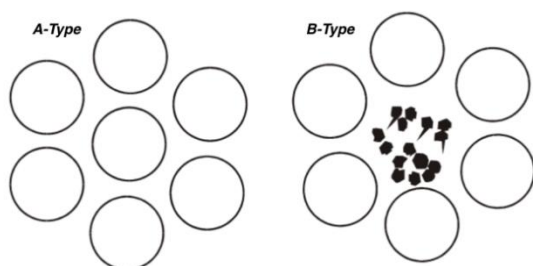


Figure 2. Brief description on cross-section of double helices in A-type and B-type starch granules. Black points show water molecule.

Some plants like peas granules are with both A- and B- type pattern assigned together which is named as C-type. In A-type crystallite, the double-helices are tightly and strictly packed into monoclinic unit cell (dimensions at $a= 20.8 \text{ \AA}$, $b=11.5 \text{ \AA}$, $c= 10.6 \text{ \AA}$, B2 space group) by containing 8 water molecules⁶. Differential from B-type crystal, the double-helices are settled into hexagonal unit cell (dimensions $a=b= 18.5 \text{ \AA}$, $c= 10.4 \text{ \AA}$, $P6_1$ space group) with 36 water molecules⁷. Small-angle X-ray scattering (SAXS) applied to explore the distance in starch granules, which is shown 9-10 nm repeated⁸. This was suggested to stem from stacks of repeating amorphous and crystalline lamellae, which representing as double-helices (Figure 1). Crystalline lamellae can be separated from acid-treated starch. Waxy granules with A-type crystallinity analyzed by TEM show regularly generated parallelepipedal blocks having angles of 60° - 65° and with length and width at 20-40 and 15-30 nm, respectively⁹. So that the information of dimensions suggests that one single nanocrystal contains involves 150-300 double-helices. Amylose in starch contributes rise to nanocrystals with less perfect symmetry, suggesting the interference of amylose to crystal structure. Nanocrystals isolated from B-type granules such as potato starch has irregular structures, probably resulting from the organization of double-helices in B-crystallites. Since the repeating distance is 9-10 nm and crystalline lamellae fills in 4-6 nm, the thickness of amorphous lamellae is 3-6 nm. This section has longer internal chains of both amylopectin and amylose. The amorphous lamellae seem to be thicker when amylose (such as waxy starch) is absent rather than in its presence, whereas the crystal lamellae are thinner. Molecular density

of crystal lamellae in different species are different, for instance, density of potato granule is 1.1 gcm^{-3} , whereas density of waxy maize is 1.22 gcm^{-3} , may be because of water content in B-polymorph crystals is higher, while the molecular density of amorphous lamellae is similar in B- and A-crystalline. The accumulation of crystal and amorphous lamellae constitute rings with thickness of 100-400 nm. The rings are semi-crystal naturally due to they contain both crystal and amorphous lamellae, but somehow they also are named as “crystalline” or “hard” shells. The rings are embedded into amorphous matrix, which was described as “amorphous background”. So that granular rings often named as growth rings are generally thinner at granular periphery and thicker at interior parts. In the center of granule, the region was named hilum, which was surrounded by void (filled with water if starch granules not dried) when growth ring was absent¹⁰. In cereal starch granules, there are channels penetrate granules from surface, whereas channels here connect surface to interior voids, if present¹¹. These channels are filled with proteins and phospholipids, which are significant to the processes reacted by α -amylases or glucoamylases, even for the industrial applications such as chemical modifications. On the surface of granules, protrusions can be found by SEM and AFM, with size between 10-300 nm, named blocklets. Besides on the surface, blocklets are also observed within the growth rings at the interior regions of starch granules (Figure 1). The result illustrates that the increase of relative crystallinity shall be accompanied with water content¹². The lamellar structure can be only recognized by SAXS in the humidified particles, so the appearance of crystalline structure is turned out by the fusion of blocks. Blocky materials is detected in both amorphous and semi-crystalline rings, whereas the latter (soft rings or shell) consists of defective lumps compared with hard shell or common blocklets. Through the observation about the size of the block, a single block may represent one or several amylopectin molecules. Amylose is supposed to be a component of blocklets, which functions as the interconnecting material out of blocklets¹³. In general, starch granules contain many structural levels, from internal to dimensional structures, such as the external chains of amylopectin with double helix, crystal and amorphous lamellae, blocklets and growth rings, spans from micrometer to angstrom. The participation of linear amylose in granules is still uncertain, while

the presence of branched amylopectin is agreed with the semi-crystalline structure of granules.

1.1 Amylose

Amylose is a polysaccharide, together with amylopectin, is the main component of native starch granules, counting for 20%-30% of granule weight. In addition, amylose can be synthesized in vitro by enzymatic ways. As referred above, amylose is linear and slightly branched, whereas the linear property shows important effect on physicochemical properties of amylose: crystallization properties and conformation in solution, for instance. In starch granules, amylose contributes to the amorphous parts in alternation within semi-crystalline rings of amylopectin. Crystallization in vitro, amylose is more versatile than amylopectin.

1.1.1 Structure of Molecule

Amylose accounts for a relatively minor proportion in starch granules, but its morphology generally exists in the form of linear or slightly branched chain. In general, the molecular weight of amylopectin is larger than that of amylose, and moreover, the average chain length of amylopectin is shorter than that of single chain in amylose¹⁴. The molecular size of amylose varies in different kinds of starches, as shown in Table 1¹⁵. The percentage of branched amylose can be roughly evaluated by the degradation of amylose by β - amylase. The linear components were completely transformed into maltose, and the branched chain components were partially turned into maltose and β -limit dextrin containing the inner part of the original molecule and the whole branched chain¹⁶. These results showcase that the proportion of branched amylose molecules in different plants is basically specific.

Table 1. Information of amylose structure and details in different starches

SOURCE	AMYLOSE(%)	DP _n ^a	CL _n ^b	β -LV(%) ^c	N _{branched} (%) ^d	NC _{branched} ^e
WHEAT	17-34	980-	135-	79-85	26-44	12.9-20.7

		1570	270			
TRITICALE	23-27	n.a. ^f	n.a.	n.a.	n.a.	n.a.
BARLEY	22-27	1220- 1680	315- 510	76-82	21-45	6.1-13.8
OAT	18-29	n.a.	592- 907 ^g	n.a.	n.a.	n.a.
RICE	17-29	920- 1110	230- 370	73-87	31-69	5.7-9.7
MAIZE	20-28	960- 830	305- 340	81-84	44-48	5.3-5.4
POTATO	25-31	4920- 6340	520- 670	68-80	n.a.	n.a.

Note: Values represent summary from literatures^{2, 17-21}. ^a Number average degree of polymerization. ^b Number average chain length. ^c β -amykolysis limit value. ^d Molar fraction of branched amylose molecules. ^e Average number of chains in branched molecules. ^f Data not available. ^g Weight average values (CL_w).

Branched amylose has short chains with length usually attributed to amylopectin. Relative number of chains by weight is extremely low which is below detection limit by analytical devices. On the molar basis, the chains dominate in amylose, thus the tissue of short chains in amylose is different from amylopectin due to the situation of size distribution.

The chemical structure of linear amylose is illustrated in Figure 3 while the proposed structure of branched amylose is shown in Figure 4, which contains less than 1% branching points in nature.

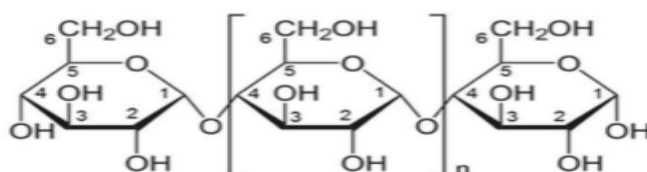


Figure 3. Chemical structure of linear amylose

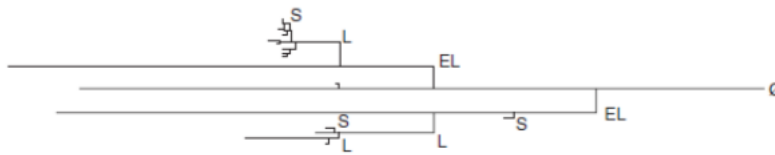


Figure 4. Proposed structure of branched amylose

1.1.2 Granular Amylose

As mentioned above, it is generally believed that amylose exists in amorphous state in starchy granules, but the true position of amylose in granules is still controversial. Starch is easily corroded when it is processed in concentrated chlorine or lithium chloride solution. When corn, potato or other starches are treated with controlled manner to achieve erosion from the surface to inside, it's easy to obtain that the solubilized parts containing granular residues²². Studies show that amylose in potato and corn starch is more concentrated near the surface than it in interior. But meanwhile, other experimental results indicate that amylose more closely adhered to the granules by detection of fluorescent probe (8-amino-1,3,6-pyrenetrisulfonic acid, referred as APTS) to the reducing end of potato, corn, wheat and barley under confocal laser scanning microscope²³. Here argue is how much the amylopectin and amylose are interrelated inside granules. When the starch is heated in water, it will expand in different degrees due to various condition of the temperature and cause the leaching of amylose. In this process, amylose is easy to lose to hot water²⁴. Results suggest that amylose in corn was more easily lost than that in potato. Therefore, experimental results explain that amylose in potato is connected to amylopectin strongly, while amylose in corn, rice, wheat and other starches has less correlation with amylopectin. In addition, amylose can be crosslinked with amylopectin in starch granules to disperse amylose between amylopectin molecules in corn and potato starch. As far as the granular layer structure is concerned, amylose affects the SAXS analysis of wheat granules, so it can be determined that amylose and amylopectin can pile up the lamella together²⁵. As articulated, amylose has defects in starch granules such as wheat, rice, potato and so on, and entered the crystal area to affect the stability of starch crystal.

1.1.3 Helical Conformation

Best way to explore amylose was by concentrated 0.5MKOH, DMSO, or 6-8 M urea. When the pH value is greater than 13, the hydroxyl groups on the glucose residues change negatively, and the molecules extend to the maximum volume. In aqueous solution with a neutral pH value, amylose exhibits an extended random coil, a random one with a helix segment extending or a wormlike helical conformation. As widely discussed, amylose is not stable in aqueous, in particular, the amylose B is not stable in water²⁶. Not only amylose clots but also single amylose molecule can form the helix. These molecules can easily interact with fatty acids, iodine or different alcohols to form inclusion complex²⁷. Left-handed helices are tighter than double-helices, whereas in turning of helix may contain 6-8 glucosyl units relying on the guest molecule. Single amylose helices could crystallize into the special pattern called V-polymorph²⁸. XRD analysis revealed starch granules often show characteristic peak at $2\theta=20^\circ$ to contribute to V-amylose-phospholipid complexes. But peak at $2\theta=20^\circ$ can be also found in other low amylose, even amylose-free starch, so it cannot be solely concluded to amylose-lipid complexes²⁹. Therefore, amylose can be sorted into lipid-complexed and free amyloses. The most common method to do quantitative measurement on amylose in granule is blue coloration of starch with iodine to get iodine-amylose complex. Due to lipid-complexed amylose interferes with measurement, so only free amylose is detected. Starch samples need to be completely defatted to get the total amylose content³⁰. Then lipid-complexed amylose can be estimated by indirect method based on the total amylose content and free amylose. By forming helical complex with lipids and other compounds, amylose-lipid complex shows hydrophobic moiety. The single-helical complex of amylose (inclusion complex) has hydrophobic portion of complex agent presented in the hydrophobic cavity of helix³¹. Size of lipids-amylose complex depends on the cross-section diameter of complexing agents: 8 glucose units per turn for compounds with even bulkier cross-sections, like $C_{10}H_{18}O$; 7 glucose units in one turn for compounds with branched chains, such as C_3H_8O and C_2H_6OS ; 6 glucose units per turn for compounds with linear hydrocarbon chains (e.g. n-butyl alcohol and free fatty acids)³². Lipids could produce helical-complex with amylose containing monoglycerides,

phospholipids, free fatty acids and long-chain alcohols. The formation of amylose-lipids complex in starch granule affects granular properties like gelling, pasting and digestive in animals and humanity. Normal corn starch exhibits higher pasting temperatures and lower peak viscosities compared with waxy corn starch, the reason causing this difference is because the normal corn starch has around 1% endogenous lipids, while waxy corn starch has less lipids³³. The combination of lipids and amylose in normal corn starch restrict the swelling of starch particles/granules and prevents the dispersion of expanded starch, which is a necessary condition for starch gelation happening.

1.2 Amylopectin

Amylopectin (molecular mass: 10^7 - 10^9 g/mol) is highly branched with average degree of polymerization (DP) extremely various, whereas amylose is linear or slightly branched with less varied DP and molecular mass of 10^5 - 10^6 g/mol which is easily form single or double helices, so that amylopectin is one of the largest molecules in nature³⁴. Researches also indicate amylopectin molecule from different sources consist of three size-fractions with average DP ranging at 700-2100, 4400-8400 and 13400-26500, of which large molecules predominate. The polymeric connections in amylose is linear in which glucose residues are α -D-(1-4) linked, while amylopectin exists with both linear and branched chains at α -D-(1-4) and α -(1-6) glycosidic bonds, respectively. Amylopectin and amylose are kept as granules from sub-microns to 100 μ m in diameter. Amylopectin is the major component in starch, mostly comprising 70%-80%.

1.2.1 Categories of Chain

As mentioned, an amylopectin has many side chains with shorter length than the main chains of amylose. The size distribution of chains can be analyzed by fluorophore-assisted carbohydrate electrophoresis or high-performance anion-exchange chromatography. Chains in amylopectin can be categorized as two: long chain and short chain. The molar ratio between the two chains varies with the type and source of starch. Generally, this proportion is the largest in cereals, as shown in Table 2.

Table 2. Lengths and ratios of the chains in amylopectin

SOURCE	STRUCTURE ^a	CL	ELC	ILC	TICL	S:L	BS:BL	A:B
Oryza sativa	A:2	16.9	10.7	12.4	5.2	14.2	5.4	1.0
Maize	A:2	19.7	13.1	12.6	5.6	9.9	6.3	1.1
Wheat	A:1-2	17.7	12.3	12.7	4.4	16.2	6.8	1.4
Oat	A:1	17.0	10.7	12.6	5.3	18.2	8.6	1.0
Potato	B:4	23.1	14.1	19.9	8.0	6.3	2.3	1.2

Note: Values represent the summary from literature³⁵⁻⁴⁰. CL: Average chain length; ELC: External length of chain; ILC: Internal length of chain; TICL: Total internal chain length; S:L=Ratio between short chains and long chains; BS:BL=Ratio of short to long B-chains; A:B=Ratio of A- to B-chains. ^aType of granular crystal structure and type of amylopectin molecular structure.

As mentioned above, short chains forming double helices are involved in crystal formation in granules. Short chains are berthed on long chains, so that being the interconnecting chains and confined to amorphous lamellae. Chains in amylopectin are named as: A-chains; B-chains are substituted with other names to distinguish more meanings; and the macromolecules of C chain embraces a single reducing end group, being similar to B chain. The long B chain can be divided into B2 chain (DP 42-48), B3 chain (DP 69-75) and longer chain. The main chain group of short chain includes A-chain and B-chain, which is called B1-chain. In addition to short chain and long chain, several amylopectin molecules contain extra-long chain (EL chain), also known as super-long chain. EL-chains consist of several hundred or thousand glycosyl units to form the type like amylose chains and hard to distinguish from amylose.

Generally, EL chain is composed of hundreds of thousands of glycosyl units, during the formation of amylose. That's why EL chains are hardly to be divided from amylose.

EL chains exist in Indian rice varieties, but not in japonica rice varieties, and also in potato, wheat, cassava and barley⁴¹.

The C-chain of amylopectin was widely distributed between DP 15-120, and the peak value was at DP 40⁴². The length of the C-chain varies from molecule to molecule because of an amylopectin molecule contains only one single C-chain.

The boundary of the outer chain is described as a segment extending from the outermost branch of the chain to the non-reducing end. According to this definition, chain A is completely external, but B-chain has only one external segment while others are all internal.

The whole inner chain from the outermost branch of the chain to the reducing end side is considered as the inner chain, and if the outermost branch residue is not included, this chain is the core segment⁴³.

Most of the segments embedded into multiple branches are defined as internal segments, and their average length is the only measurable inward parameter of the latter. To understand the internal chain structure of amylopectin, the outer chain must be removed. β -amylase and phosphorylase a (enzymes in the liver and muscle involved in glycogen metabolism) are commonly used to analyze the internal chain structure. However, phosphorylase can remove a glucose residue from the non-reducing end to produce glucose 1-phosphate through phosphorylation mechanism, while β - amylase produces β -maltose by hydrolysis, as described above⁴⁴. None of these two enzymes act on branches. Phosphorylase a generates ϕ -limit dextrin, where all A-chains reduce into maltotetraosyl stubs⁴⁵. When ϕ -limit dextrin hydrolyzed by β -amylase, apiece chain is reduced by one additional maltose residue, so that the A-chain is retained as maltosyl residue, which is called ϕ, β - limit dextrin⁴⁶. The length of the outer residue of β - limit dextrin depends on whether the original outer chain consists of even or odd number of glycosyl units, rather the DP of A-chain is 2 or 3. The analysis of inner chain can be realized by enzymes like pullulanase and isoamylase. The results illustrate that the two enzymes had instinctive hydrolysis effects on different substrates: pullulanase had better hydrolysis effect on maltosyl segments, whereas isoamylase shows better hydrolysis effect on whole amylopectin. The glucosyl branched chain is resistant to both of these two enzymes. The ratio between chain A- and B- chains is usually at 1.0 and 1.4. The short B-chain in the

internal chain profile can be settled into two subgroups: B-chain (B_{fp}) is considered as the typical "fingerprint" contour in the chromatogram based on plant origin and source, and the main group of BS-chains (BS_{major}). The internal BL-chain can be divided into two subgroups: B2- and B3- chains, which is the unit chain of amylopectin. And, two types of A-chain are detected, the shortest chain in the unit chain profile of amylopectin (without external chains removing) at DP between 6 to 8 are considered as A-chains, called "fingerprint", analog to B_{fp} -chains having similar typical profiles in chromatograms but shorter. The remaining of A-chains is considered to be crystal A-chains (referred as $A_{crystal}$) since it had chains with $DP < 9$ that cannot form double-helix with other chains⁴⁷. Therefore, the unit chain of amylopectin is used to estimate the average length of chain. Via combing the information from internal and unit chain profile, internal, external, total and average chain lengths could be calculated, shown in Table 2.

1.2.2 Branch Units

As discussed in 1.2.1, chains in amylopectin are set and embedded into diverse groups whatever small or large can be isolated by endo-acting enzymes. Although various endo-acting amylolytic enzymes exist, used for structural analysis is very few. Such as α -amylase of *Bacillus amyloliquefaciens* is used mostly used to investigate the branched structural parts of diverse amylopectin by far. *B. starch oligosaccharide* α -amylase shows the most obvious internal-action pattern and finally is utilized to isolate the larger branched α -dextrin from amylopectin. There are nine sub-sites surrounding catalytic site in *B. amyloliquefaciens* α -amylase. This enzymatic reaction happens only at the sub-sites with glucosyl units. During the reaction, the reaction rate is very fast initially because long chain segments contained in substrate are completely filled up sub-sites. Later, reaction doesn't follow this method, resulting big reduction in reaction speed. α -Dextrins generated during this stage could represent the unit clusters of chains. Due to the property of sub-units in enzyme, the internal chain segments among branches in the clusters isolated is DP smaller than 9, which presenting the structural definition of cluster. Groups of clusters called domain can be isolated through interrupting the hydrolysis before the initial stage finishes.

Since α -amylase attacks the external chains in amylopectin out of controlled state, thus the external segments showed diverse lengths and can be removed by phosphorylase or β -amylase. The dimensional distribution of clusters is quite wide, changing from DP 15 to more than 500, which is based on origin of amylopectin. In type 1 and 2 amylopectin, the largest clusters are found with average size around DP 66-73, which is corresponding to the average number of chains (referred as NC) around 11-14⁴⁸. Different starch shows various NC of numerical value range, as Table 3 illustrates. Isolated dextrin can be formed after enzymatic treatments. Compared with original amylopectin, the number of long chains is decreased, and the domain size was smaller than the cluster structure. It indicates that α -amylase works on the long inner chain. After producing new shorter chains, some of them are similar to the ones existing in amylopectin and others represent to other classifications, which are very important in the grooves of chromatographic characteristics of short and long chains of amylopectin.

Table 3. Structure of intermediate clusters (α -dextrin) isolated from amylopectin by α -amylase of *B. amyloliquefaciens*.

Starch	Structure ^a	NC	CL	ICL	TICL	IB-CL	NBbl	Molar Distribution of Building Blocks (%) ^b				
								2	3	4	5	6
Asian rice	A:2	12.0	6.8	4.7	7.9	6.9	5.7	50	29	11	9	1
Africa rice	A:2	14.1	5.9	3.8	7.9	6.5	5.1	40	29	13	14	4
Maize	A:2	12.5	5.4	3.3	10.5	6.2	4.2	51	27	10	12 ^c	
Wheat	A:1-2	14.2	5.8	3.6	11.9	6.4	6.3	57	24	10	8	1
Rye	A:1	11.5	6.1	4.0	10.5	5.9	5.5	55	28	9	7	1
Oat	A:1	11.8	6.1	4.1	10.4	5.7	5.7	55	27	9	7	2

Note: values cited from literatures⁴⁹⁻⁵². NC: average number of chains in cluster; CL, ILC, and TICL are referred in Table 2; IB-CL: inter-block chain length; NBbl: average number of building blocks in cluster. a, Type of granular crystalline structure

and type of amylopectin molecular structure. b, Building blocks of group 2 have two chains, group 3 have three chains, and so on. c, Total percentage of group 5+6.

The obvious clusters isolated from amylopectin are extremely slow to be hydrolyzed, when treated by α -amylase finally into small α -limited dextrin, which constitute to the branched units called building blocks. However, definition of building blocks can be explained to the composition of various groups of α -limited dextrin with number of chains increasing. Thereby group 2 consists of building block with two chains with DP 5-9, group 3 have three chains with DP 10-14, and group 4 have four chains with DP 15-19⁵³. Since the complication of each group raises with size, the larger building blocks are isolated as course preparation. Finally, group 5 comprises dextrin with 5-7 chains (average 6) and group 6 have 10 chains with DP>35.

Group 6 represents a few ratios or less of blocks with similar size distribution, regardless of the structural type of amylopectin, as shown in Table 3. The largest building blocks in group 6 contains the same block found in most clusters. However, chains in building blocks are shorter than those in clusters (11% - 15%) and branch density is higher (14% - 20%) because of the short distances among branches, which have internal chain length 1.4-2.3. Data in Table 3 recommends that the inter block segments, as well as inter cluster segments play important impact on the thermal properties of starch. The chains in clusters interconnecting building blocks named B-chains consist of intra-block and inter-block chain segments. B-chain explains a number corresponding to counts of inter-block segments along the chain, as Figure 5 shows⁴⁸. Thereby B0-chain lack internal block segments due to they are all inside building block. DP of these chains is between 3-6, and corresponds to B_{fp}-chains in original amylopectin if not completely treated by α -amylase. B1-chain has one inter block segment with DP 7-18, and can be divided into B1a-chain (DP between 11-18), with a segment at reducing-end side, which probably has up to 6 glucosyl units which spreads among building blocks. B2-chain with DP between 19-27 contains two inter block segments to expand via building blocks. Eventually B3-chain (DP \geq 28) contains more than three inter block segments. So that each building block in A- and B-chains contribute with intra-blocklet segment (DP 5-6), as well as inter blocklet segment (DP

5-8) connects to next block.

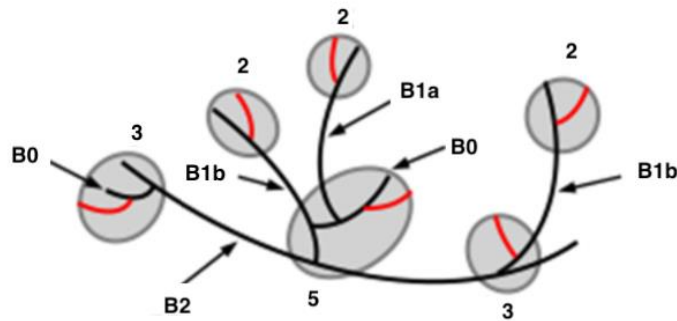


Figure 5. Types of Chain and building blocks in cluster. red and black lines represent a- and B-Chains, respectively. B-chains are numbered based on the number of inter block segments. Grey color encircled stands for building blocks and numbered according to the chain numbers.

1.2.3 Structural Types of Amylopectin

Internal chain contour of amylopectin is specific for various plant, which is classified into four types to explain the distinctive structures. Type 1 amylopectin is representative for some particular cereals: oat, barley and rye. Type 2 amylopectin contains more B-chains than type 1, and typical starch has type 2 amylopectin is: rice, maize and pseudo-cereal amaranth. Type 3 amylopectin includes mung bean and cassava starch has less “finger print” B-chains than type 1 and 2. Type 4 amylopectin contains all B-crystalline starches such as edible canna and potato granules, owns highest amount of B3-chains.

1.2.4 Tissue structural units in amylopectin

It's hard to establish a meaningful mode to explain the structure of amylopectin due to many pieces of information like the internal chains, form of unit chains and diverse branched units with composition of chains. Two modes are mostly accepted: building block backbone mode and cluster mode.

Building block backbone mode is the latest model based on experiments. In this mode, amylopectin has L-chains connecting to each other to generate a backbone

longer. The building blocks are extended among the backbone to form the integrated section, which is characterized as internal. The building blocks distribute along backbone randomly. In some amylopectin with type 1 structure, some longer short B-chain is also embedded in backbone. The short B-chain here may generate shorter branch of backbone to link to building block outside named external building block, however some starch may contain long branches expanded from backbone. In starch granules, short chains construct double helices of crystal lamellae, shown in Figure 6A¹⁵. The backbone is inlaid in amorphous lamella and spreads among it instead of passing through stack of lamellae in the growth ring of semi-crystalline. Obviously function of inter-cluster segment is interconnecting building block, which is same to inter-block segment. Thence the branched structural units in the mode are building blocks. α -dextrin generated from starch treated by α -amylase is actually the early step of hydrolysis, so that is only apparent cluster, which is formed through prioritized attack at inter-block segment with DP bigger than 9. Based on this model, shorter chains such as B1- and B2-chains in α -dextrin have periodicity. Thus backbone model illustrates the phenomenon of the ratio between short and long chains in amylopectin. Actually backbones from molecules may cross each other to achieve intricate network. Double helices expand from the network into crystal lamellas. So that double helices from molecules gather to crystallize into A- and/or B-polymorphic pattern. Dimensions of nano crystalline isolated from granules hydrolyzed by mild acid and segregated from crystal lamellae are extremely large compared with double-helices. Network of backbones in amorphous lamellae contributes with double helices to generate crystallites in cooperative profile. It is noticed that very limited combinations of internal chain lengths result to parallel arrangement between two adjacent double helices in macromolecule. This combination is very few so that double helices from single cluster contributes to crystalline structure. Building block backbone model relatively possesses open structure: usually the most common building block is considered to have 50% of all blocks and around 25% of all branches, with only one branch and two chains. Bilateral sides of single branch are captured by inter cluster or inter block segments. The open structure would be flexible, whereas long segments could shift and turn freely compared with the compact branched clusters, leading to the ordered A- and B-crystalline. Furthermore,

the flexible segments are piece of complicated network of amorphous lamellae, which is useful for understanding the swelling of granules in hot aqueous environment. When granules heated in water, water molecules are absorbed into granules, so that the double helical construction in crystal lamellae is destroyed during a process with increasing pressure on crystallites, thus nothing prevents granules from swelling. Without absence of amylose, starch structure is stable due to it intermixes with backbone of amylopectin in amorphous lamellae to reduce the flexibility and retard swelling. Due to the proposal of building block backbone model, it is also suggested amylopectin expresses like side chain liquid-crystal, which considers the double helices are connected with amorphous backbone of cluster by flexible spacer arms. Spacer arms' flexibility illustrates the behavior like gelatinization and annealing. The inter block segments stands for flexible arms in backbone model, expressed as: the longer segments, the better flexibility. Helical structure of backbone model

Cluster model was proposed in 1969 by Nikuni and French in 1972 independently. Short chains in amylopectin become clusters interconnected by long chains, shown in Figure 6B. Four findings promoted the proposal of cluster mode: (a), granules treated by acid could move amorphous parts, while the crystal sections mostly kept. Molecular size-distribution analysis in remaining residues of granules demonstrate that main section of dextrin is linear chain with DP 13-16 and most of branch is removed, which recommends the branch is limited to amorphous parts to connect short chain in crystal area. (b), periodic length of 9-10nm detected by SAXS confirm to one crystal and amorphous lamella, whereas the thickness of former matches DP of short chains in starch treated by acid. (c), GPC (Gel-permeation chromatography) illustrates amylopectin consisting of two primary groups of chains: short and long chains. (d), cross of polarization inside starch particles demonstrates that amylopectin molecules here are arrayed radially with chains indicating to same direction toward the granular surface.

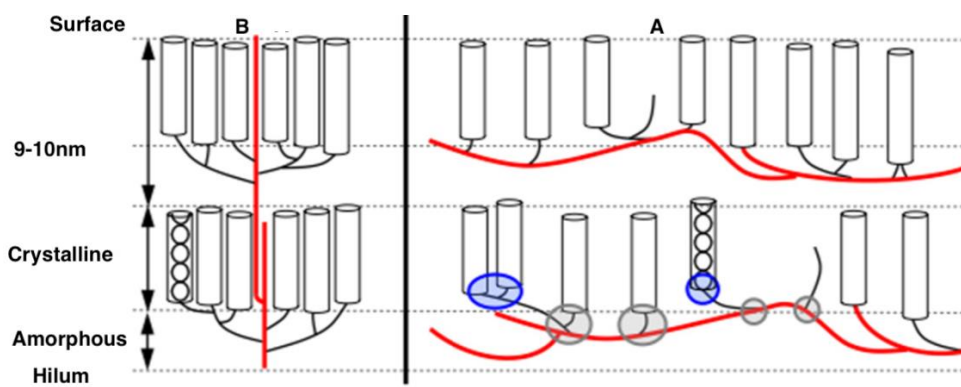


Figure 6. Amylopectin inside semi-crystal growth ring described by building block backbone mode (A) and cluster mode (B). Amorphous and crystal lamellae are shown by dotted grey lines. The thick red and black lines represent long and short B-chains, respectively. Backbone in A carries the internal building blocks (encircled in grey) and major short B-chains which take shape distributing from branches to backbone to connect to external building blocks (encircled by blue). Cylinders represent the double-helices generated by external chains. Single grey chains mean defects in crystal lattice.

Experiments of amylopectin treated by maltotetraosyl generating enzyme, cyclodextrin glycosyltransferase and α -amylase illustrates dextrin was the cluster in amylopectin. Periodicity of the chain length with 27-28 glucosyl units through B-chain of amylopectin was confirmed to correspond to periodic length between 9 to 10nm, also the inference of B2- and B3-chains contain two and three clusters, respectively. Through comparing unit chain of range in amylopectin, periodicity of chain length for 12 glucose residues is in short chains instead of long chains. Molecular model showed amorphous chain segments included in interconnecting double helices of crystal lamellae into parallel array having various and perpendicular directions to helices. Cluster model forecasts the isolated clusters remain short chains due to the long chains must be cleaved for the release of clusters from macromolecule. Even though short chains are mostly contained in isolated clusters, there are still few long chains in it, whereas number of long chain reduces compared with original amylopectin. The ratio between short and long chains could estimate the average number of chains from isolated clusters, which is lower than theoretical value. Average number of chains from isolate cluster in B-crystalline starch, which

contains amylopectin with type 4 internal structure corresponds the inference of cluster model. These information results that building block backbone model matches the experimental data better than cluster model.

1.3 Lipids and proteins

Starch contains endogenous lipids, which depend on plant species. Lipids associated with various starch granules happen both at surface and inside. Lipids in two positions are different in extractability from granules by fat solvents. Ether lipids on surface can be extracted by aqueous alcohol but not diethylether. Lipids on surface are mainly triglycerides, followed by free fatty acids, glycolipids and phospholipids, whereas internal lipids are mostly monoacyl lipids with lysophospholipids and some fatty acids. Lipids in starch are both in free state and bound to starch components through amylose complexes, linkages via ionic or hydrogen bonding to hydroxyl groups of starch components. Amount of lipid-amylose complex ranges from 15% to 55% of amylose fraction in cereals. Formation of amylose-lipid complex is more strongly happened when granules treated by heating or moisture, especially during gelatinization process.

Proteins in granules are mostly related to biosynthesis of starch. Some proteins are loosely associated with starch, while some others are tightly bound inside granules. Starch-associated proteins are present on surface and in channels of starch granules, which are called granule-surface and granule-channel proteins. Molecular weight of these proteins are around 5-148 kDa, whereas low molecular weight proteins on surface are residual zein proteins. Method to distinguish botanical origin of starch is by observing the way of starch-associated proteins crossing starch. Hydrolysis of starch started began from channels, following the pattern from interior to exterior, and the degree of digestion depends on the structure of starch where function of proteins on surface act as α -amylase inhibitors through providing competitive binding sites for amylase. And the proteins in channel would have greater effect with amylase than proteins on surface, which lead the initial digestion beginning from channels. After proteins in channel were moved, amylase selects active sites on surface to bind rather than starch matrix, causing less digestion of starch. Furthermore, proteins in channel probably conduce to structural stability of granule by interactions between proteins

and starch. Surfaces of granules play a role to obstruct the attack from enzyme and chemical reaction, whereas proteins on surfaces is related to pasting property closely. Digestibility of starch is largely decreased while starch-protein is lacked, showing that proteins stabilize granular structure significantly. Probably there are two mechanisms of function from proteins in granular channels on starch digestibility: (1) lack of proteins in granular channels may magnify channels causing hydrolysis by amylase easier; (2) reactive positions at granule-channel proteins are prioritized for α -amylase to attack. The missing of proteins in granule is dramatically weaken structure of starch, and expose the surface of starch to enzymes.

1.3.1 Properties of starch

1.3.2 Swelling

As the most important and significant property, The swelling of starch granules triggers out the separation and crystallization loss of amylopectin, which promotes the leaching of amylose and creating space to inner granule structure. Because of the strong hydrogen bonding, starch granules are insoluble in cold water. But, when the starch particles are heated aqueously, the semi-crystalline is destroyed. Water molecules turns to combine with the hydroxyl groups at the ends of amylose and amylopectin through hydrogen bonds. First swollen region is amorphous area, leading to disruption of radial organization. Secondly heating process causes disruption in crystalline regions, but granules are still held together. This behavior directly causes swelling and granular size increasing. Swelling capacity of starch explains the interaction of polymeric chains containing crystal and amorphous fractions. As discussed above, the extent of interaction is effected by amylopectin-amylose ratio and the features of molecules are based on the length and grade of chain branching, polymerization degree, molecular weight and configuration. Swelling capacity of granule is related to amylopectin due to amylose serves as an inhibitor and diluent of swelling. Actually swelling is the initial step of all other paste characteristics. At first step of swelling, volume of starch granule could increase up to 30%, which is reversible. Heating of starch accompanied with water absorption breaks the hydrogen bonds corresponding to granular cohesion. Water permeates the

interior of granule to hydrate the linear fragments of amylopectin. This process would lead to irreversible swelling and increase the granular size many folds and paste viscosity if water environment provides appropriate period and high temperature. The swelling power of starch can be easily calculated by equation below:

Swelling power (g/g) = weight of wet sediments / weight of dry starch

1.3.3 Gelatinization

Essence of starch gelatinization is a process of transition phase when granules heated in sufficient water surrounding, whereas different starch species have specific temperature intervals for gelatinization. Gelatinization happens when water penetrates into granules, and then granules swell depending on the hydration of amorphous to lead to loss of crystallinity. Discussion from space, gelatinization begins in hilum and extends throughout the periphery, or saying it starts initially in amorphous area, where weak hydrogen bonds presents. And then this expansion continues to crystalline region. Amylose decreases the fusion point in crystal area and energy needed to originate gelatinization. Gelatinization is evaluated by transition temperature and gelatinization enthalpies in paste, which are specific for each species. High transition temperature represents high degree of crystallinity and stability, and resistance of granular structure to gelatinization. During gelatinization process, birefringence and crystalline order is lost due to the leaching of amylose and breaking of double helix in crystalline. Structure of starch experienced gelatinization change from semi-crystalline to amorphous.

The mechanism of starch gelatinization is associated within molecules, which occurs by hydrogen bonding between O-6 of amylose and OH-2 of amylopectin, as shown in Figure 7⁵⁴. Water molecules, at the same time, is involved by four hydrogen bonds to attend the reaction, two of which include two hydrogen and two lone pair electrons of hydrogen and oxygen of two adjacent water molecules. Due to the high kinetic energy of short-side chains (A and B1) in amylopectin, its tetrahedron indicates the bonding of water, and the part of water is involved in gelatinized starch solution.

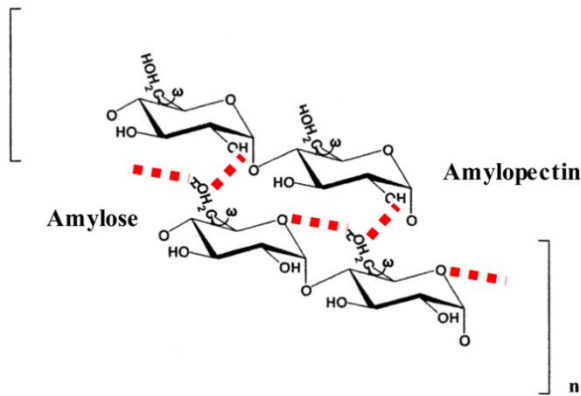


Figure 7. Gelatinization mechanism of starch. Dotted red lines mean hydrogen bonding

A and B1 short chains participate in intermolecular associations, whereas the hydrogen bonding between amylose and amylopectin is thermally stable. Because of the content proportion of amylose and amylopectin in starch is around 19%-23% and 77%-81% respectively, not less than two short side chains associate with one amylose molecule.

With appropriate temperature and time, starch granules swell until some components are in solution, the medium changes from the easy starch suspension to paste. Viscous dispersion of granules and dissolved molecules will ultimately turn into viscous starch solution, which is called gelatinization, as Figure 8 shows⁵⁵.

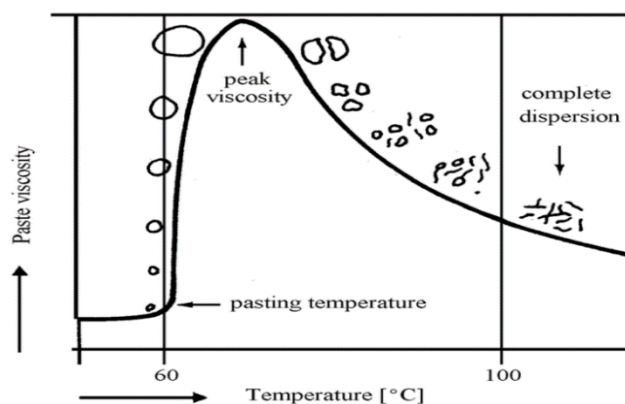


Figure 8. Gelatinization of starch experienced swelling, disruption and dispersion

1.3.4 Retrogradation

Starch gelatinization in aqueous condition is a procedure on break down of intermolecular association between amylopectin and amylose in granules with heating. High viscous solution is generated after gelatinization and transforms to strong gelling state on storage for long time, which is called retrogradation. Retrograded starch showed lower enthalpy than native one because of the weaker crystallinity in retrograded starch. The transition temperature of retrograded starch is lower than gelatinization temperature, due to the recrystallization of branched chains in amylopectin exists in less ordered situation in stored gels. During retrogradation process, amylose and amylopectin show different roles and functions. Retrogradation of amylose is a relatively fast event compared with amylopectin retrogradation. Retrogradation of amylose undergoes multi-stage process, where formation of helices and rapid formation of crystalline amylose regions happened firstly, and much faster than amylopectin retrogradation. After gelatinization, amylose is in random coil formation, whereas a gel network rapidly created by double helices formation through reordering process. By comparison the retrogradation of amylopectin occurs over longer period than amylose, which is because of the linear structure of amylose. Due to branched structure of amylopectin, once helices formed, they connect to main polymer chain by α (1-6) branch points through aggregating to generate crystals, hence the range of bond energy for main chain and segments at branching points could decrease. Mode used to describe retrograded starch is chain-folded polymer model through the crystallization kinetics developed for synthetic polymers. Crystalline regions in chain-fold polymers are composed by lamellae, where chains are located at adjacent positions, perpendicular to surface of lamellae. Based on chain-folded polymer model, the double helices could form crystallinities, whereas the “folds” are composed by branching regions, although retrograded starch is not real folded polymer. For retrogradation process, fiercer intermolecular hydrogen bonding happens both between amylose and amylopectin, as well as among amylopectin. When the intermolecular hydrogen bonding between amylose and amylopectin finished, the association among amylopectin would happen by hydrogen bonding

subsequently. The bonding in retrogradation process is because of the decrease of kinetic energy and Brownian motion of water throughout amylopectin⁵⁶.

2. Vancomycin

To be first discovered from soil sample in interior jungle of Borneo in 1950s, vancomycin was used limitedly due to the presence of impurities that caused toxicities in early preparation. However, after the emergence of methicillin-resistant Staphylococci in 1970s, the usage of vancomycin increased from the purer preparation of vancomycin was achieved in late 1970s⁵⁷. And now vancomycin has become the most common injectable drug of choice to treat methicillin-resistant Staphylococci and drug resistant Enterococcus species. Vancomycin is a large glycopeptide compound with molecular weight of 1448 Da in which inhibits the late stage in bacterial cell wall peptidoglycan synthesis⁵⁸, chemical structure is showed in Figure 9⁵⁹. The three-dimensional structure of vancomycin contains a cleft that suits by hydrogen bonding with peptides of highly specific construction of L-alanyl-D-alanyl found in cell walls of bacterial, and finally is selectively toxic by forming stable complexes⁶⁰.

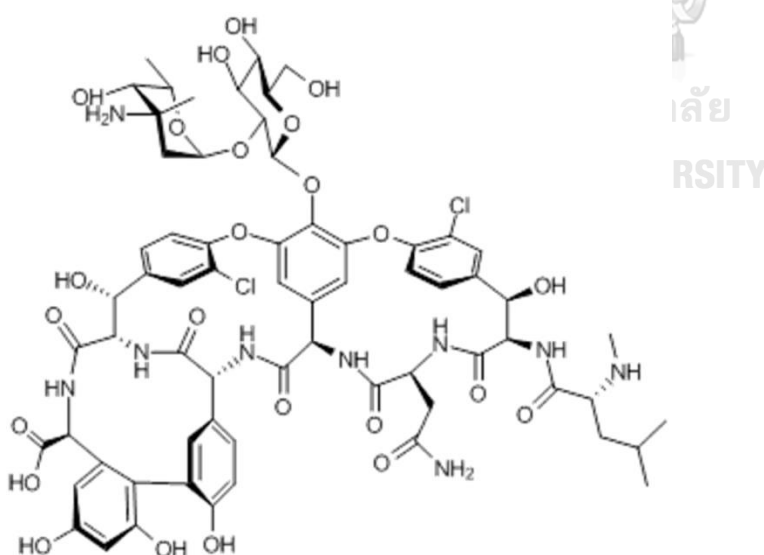


Figure 9. Chemical structure of vancomycin

Amino acids present in vancomycin are synthesized, cross-linked and joined together to assemble vancomycin⁵⁹. The main mechanism of vancomycin is by exhibiting the bactericidal activity through inhibiting cell wall synthesis against anaerobic and aerobic Gram-positive bacteria⁶¹. Vancomycin could act against most strains of Clostridia, almost all strains of *Staphylococcus aureus*, and Viridans group Staphylococci and Enterococci, but not effective to Gram-negative bacteria⁶². As the last alternative, vancomycin is used only after treatment with other antibiotics has failed in the treatment of life-threatening infections by Gram-positive bacteria, because of its high cost and continuous intravenous infusion⁶³. Improper use of antibiotics is largely responsible for the resistance problems, and due to it is the last resort antibiotic in humans, the dosage of using is limited.

Nowadays, vancomycin is used in the treatment of patients with orthopaedic implant related infections, which caused from Gram-positive micro-organisms and not susceptible to either antibiotic of penicillin class (like benzylpenicillin, amoxicillin, flucloxacillin) or clindamycin. Bone grafts are widely used in orthopaedic procedures, and by encapsulation of antibiotics with artificial material of bone to achieve the release, such as vancomycin⁶⁴.

Prolonged intravenous use of vancomycin may lead to thrombophlebitis, rash, fever, ototoxic reactions in animals and humans, so it has to be administered intravenously in diluted form due to it is highly irritable for tissues. Vancomycin may cause phlebitis at the injection site in animals, so that vancomycin should be infused for more than 1 hour to reduce the risk of histamine release-associated syndrome in humans. The drawback of vancomycin during using is damage to auditory system in humans, but the deafness and tinnitus would be relieved once treatment stopped. In addition, phenomenon like chills, phlebitis, nausea, wheezing, urticaria, and pruritus could be observed with treatments by vancomycin in humans⁶⁵. And neutropenia was also detected with prolonged therapy⁶⁶.

The colonic delivery of drugs encapsulated into carriers is useful to locally treat intestinal infections, including those caused by parasites and bacteria. Cerchiara et al. produced chitosan-based nanoparticles by ionic gelation and nano-spray-drying, to be used for colonic delivery of vancomycin to treat intestinal infections. With the aim of

improving intestinal permeability through oral administration, vancomycin biodegradable nanoparticles and microparticles were investigated with encapsulation efficiency at around 72%⁶⁷.

The organism *C. difficile* is a Gram positive spore forming obligate anaerobic bacterium and infection it causes, *C. difficile* infection is a toxin-mediated disease in intestine. The clinical results range from asymptomatic colonization to mild diarrhea and in severe cases, inflammatory lesions and formation of pseudomembranes in colon, bowel perforation (toxic megacolon), sepsis, shock and even death⁶⁸. *C. difficile* is only sensitive to the three common antibiotics in market: Metronidazole, Fidaxomicin, and Vancomycin, the dosage and acting period of vancomycin during treatment by utilizing these antibiotics may cause the high rates of recurrence and re-infection⁶⁸.

Due to the risk and side effect of vancomycin when utilized clinically, the most common method is still by injection recently, whereas the encapsulated vancomycin is not used frequently due to the high cost of production, hard to control the release, etc. Especially for the treatment to the bacterial infection in colon, carriers encapsulated with vancomycin could be delivered to the targeting position by oral would help reduce the sufferings of patients. So a convenient and low cost method to achieve the encapsulation of vancomycin is necessary in the pharmaceutical fields.

3. Edible Oil encapsulation

Encapsulation strategy to trap and protect edible oils is mostly by wall structure, coating of sensitive liquid, solid, or gas ingredients such as flavors, vitamins, and lipids to be core materials, with protective layer called wall, which can be divided into three classifications as below:

- 1). Lipids and waxes like phospholipids, beeswax and carnauba wax⁶⁹;
- 2). Proteins: Animal based proteins such as casein, gelatin; and plant based proteins like soy, pea, and barley proteins;
- 3). Carbohydrates: Marine based carbohydrates like alginate; microbial and animal based carbohydrates such as xanthan, chitosan; plant based carbohydrates such as maltodextrin, cellulose, starch;

Various methods to achieve encapsulation of edible oils recently, and could get capsules having different particle size from nano to micro. Emulsions are used in wide variety of food and pharmaceutical products, which is a key step in microencapsulation of oil. Most common status of emulsion products are oil-in-water, water-in-oil, oil-in-water-in-oil, and water-in-oil-in-water, shown in Figure 10⁷⁰.

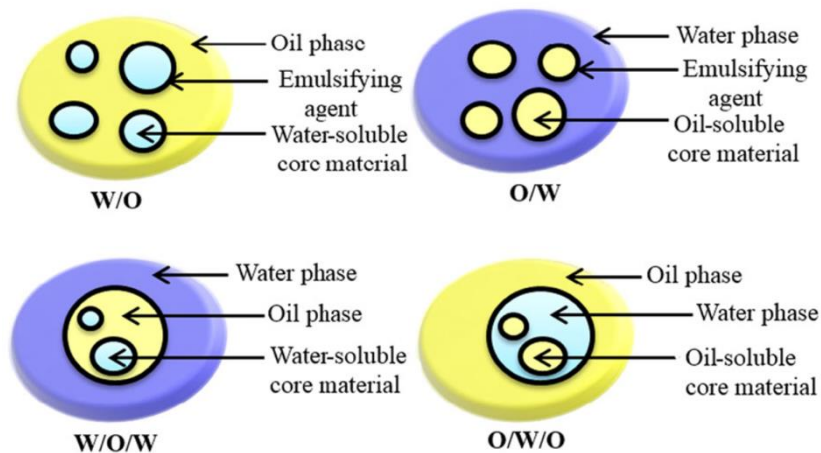


Figure 10. Illustration of the 4 emulsion systems (W/O, O/W, W/O/W, and O/W/O)

Another low-cost microencapsulation technology commonly used in industrial is spray-drying, which has attractive advantages of getting microcapsules in simple and continuous way. Spray-drying is the most common way to achieve encapsulation of oils. Equipment of spray-drying is readily available and production costs are lower than most other methods. Spray-drying involves atomization of emulsions into the drying chamber at high temperature, which leads the fast water evaporation, finally crust formed at a relatively fast rate and quasi-instantaneous entrapment of oils, illustrated in Figure 11⁶⁸.

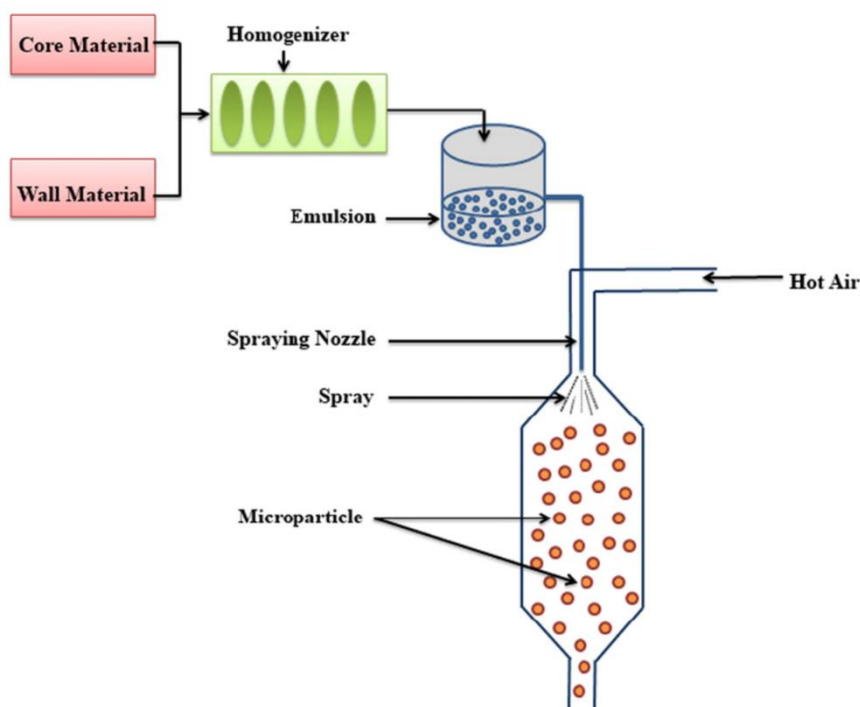


Figure 11. Schematic representation of spray-drying technology

In situ polymerization is another commonly used method for microcapsules production. It results in a formation of wall via addition of the reactant into either exterior or interior of the core material⁷⁰. Compare with other polymerization process of encapsulation, in situ polymerization is that no reactants are included into core part of the capsule. All the polymerization happens in the continuous phase rather than on the sides of interface between core and continuous phase. For instance, microcapsules entrapped tea tree oil has been reported by in situ polymerization technique, using a melamine-formaldehyde system for fragrance, the illustration to in situ polymerization is shown in Figure 12.

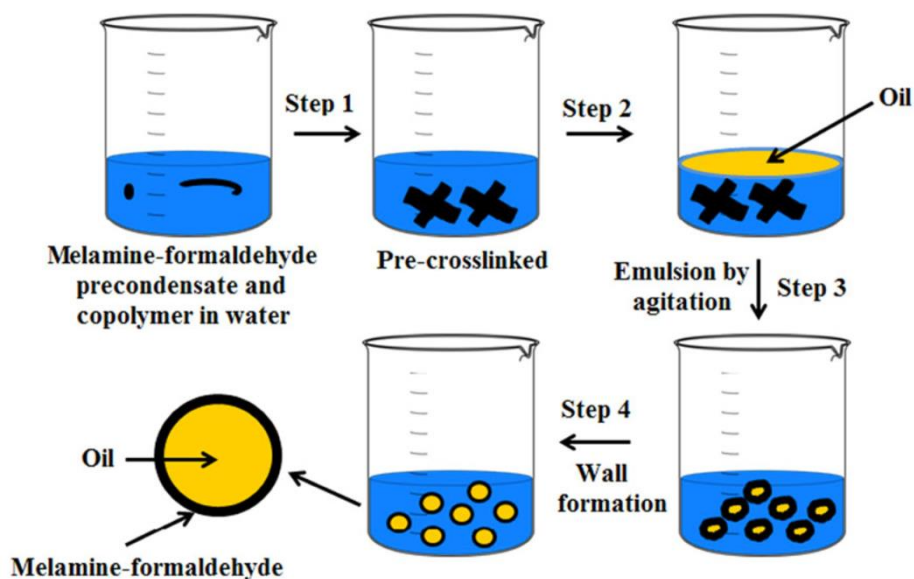


Figure 12. One example of in situ polymerization technique working on oils

Besides methods referred above, coaxial electrospray system, freeze-drying, coacervation, extrusion, supercritical fluid technique, and fluidized-bed-coating are also utilized to achieve the encapsulation of oils.

Encapsulation technologies are well-established for oil preservation. It offers a plethora of advantages, including effective protection of encapsulated oil against degradation and oxidization, easy administration, possibility of accurate control of oil release, and avoidance of evaporable components. Due to the purpose of aromatic encapsulation in food field, the product has to satisfy: food grade, good emulsifying properties, controllable release of core oils, and protect core material from environmental conditions⁷¹. All the methods discussed above are mostly in experimental conditions, but hard to amplify to industrial scales. Due to the applications of these flavors are used in food industries, a low cost and extremely easy technology to finish the oil-encapsulation is necessarily needed.

Chapter II Materials and methods

1. Materials

1.1 Starch

The rice granules (*Oryza sativa* grains) utilized in this work were all from Commercial market which were purchased from Thai Flour Industry, Bangkok, Thailand).

1.2 Vancomycin

The Vancomycin (Vancomycin-S) used in experiments were supported from 169 Siam Pharmaceutical Co. Ltd, Thailand, with white color and powdery status.

1.3 Curcumin

Curcumin, having dark yellow color (Purity \geq 98%, EC Index number: 207-280-5, Sigma-Aldrich, Singapore) was used in research.

1.4 Enzymes

α -amylase is hydrolase enzyme that catalyzes the hydrolysis of internal α -1,4 glycosidic linkages in starch to produce glucose and maltose. α -amylase can be produced using microbes by solid state fermentation which employs by products and waste products of other processes. Nowadays enzymes including α -amylase have crucial applications such as production of fructose syrup, environmentally safe detergents, and baked products. Activity of α -amylase used in thesis is having 240000 units from *Bacillus subtilis*, Sigma-Aldrich, Singapore.

Trypsin is a reagent used during manufacture of biological medical products. Porcine trypsin is an animal derived material isolated from pancreas of pigs. Trypsin utilized in thesis has 65000 units from porcine pancreas, Sigma Aldrich.

Lipase is a ubiquitous enzyme, which has physiological significance and industrial potential. It catalyzes the hydrolysis of triacylglycerol to glycerol and free fatty acids. Real lipases break down emulsions of glycerol and long-chain fatty acids, such as triphenylamine and Triallyl. Lipase used in this work holds activity at 2000 units from porcine pancreas, Sigma Aldrich.

Papain is an endo-soluble plant cysteine protease isolated from papaya latex. Papain belongs to the papain superfamily, which has strong proteolytic activity surrounding proteins, short-chain peptides, amide links and amino acid esters. The function of papain depends on its unique structure and explains how proteolytic enzymes work. Papain enzyme used in thesis has 10000 units from papaya latex, Sigma Aldrich.

1.5 Edible aroma oils

1.5.1 Sweet basil oil (SBO)

Sweet basil oil derived from leaves of *Ocimum Basilicum* botanical, which is known as Basil herb in industry. Basil herb is believed to have fortifying effect on human's mind and emotions, has been used for multiple applications including medicine, cooking, cosmetic and necessary.

1.5.2 Lemongrass oil (LO)

Lemon grass oil has a light citrus flavor and is often used in Asian dishes such as soups, teas, curries, fish, beef, poultry and seafood. Due to its unique flavor, lemongrass oil promotes healthy digestion and acts as an integral nourishing body system. It can also purify and regulate the skin, which is often used in skin care products. In Thailand, citronella oil is especially widely used in mushroom soup cooking fast food.

1.5.3 Blackpepper oil (BO)

Known for the ability to spice up meals and enhance the taste of foods, Blackpepper essential oil is a multi-purpose oil that has various uses and benefits. Sharp flavor of

Blackpepper makes it an ideal addition to meats and soups. But due to powerful chemical components of BO, its essential oil is much more than just a handy spice in kitchen. Blackpepper essential oil is high in monoterpenes and sesquiterpenes, which are natural chemicals known for their antioxidant activity and their ability to support the immune system when needed. When BO is orally ingested, a sesquiterpene called caryophyllene helps the body support healthy cell function. Internal use of BO can also promote healthy circulation, but when used topically, it should be applied with caution due to its powerful warming sensation. BO is a diverse oil that provides many physically and mentally stimulating properties essential to promoting human health.

1.5.4 Tea tree oil (TTO)

Tea Tree Oil from *Melaleuca alternifolia* contains various mono- and sesquiterpenes as well as aromatic compounds. The monoterpenes terpinen-4-ol, α -terpinene, α -terpinene, 1,8-cineole, p-cymene, α -terpineol, α -pinene, terpinolenes, limonene and sabinene account for 80 - 90% of the oil. The natural content of the individual terpenes in Tea Tree Oil may vary considerably depending on the *Melaleuca alternifolia* population used, the climate, the leaf maceration, the age of the leaves and the duration of distillation. TTO is used as aroma additive under strict dosage, such as in ice cream.

1.5.5 Kaffir lime oil (KLO)

KLO is an essential oil extracted from the leaves of kaffir lime. It has important biological activities, such as antioxidant, antileukemia, antitussive, anti-bleeding, antioxidative stress and antibacterial. Recently, KLO has been widely used in food, perfume and cosmetics industry as a spice. The oil is rich in monoterpenes (87%), and the main components are diopinene (10%) and limonene (4.7%). Mostly KLO is used in Thai foods, like fish, vegetable cakes and beef, as well as soups or curries.

1.5.6 Garlic oil (GO)

Garlic plant is used as flavoring agent and traditional medicine since antiquity. Allicin is the most predominant thiosulphate in garlic that is responsible for the characteristic odor with antibacterial effect and toxic to insects. Garlic oils are dominated by allyl polysulfides, and the organic-soluble ally sulfur compounds are present as alliin, ajoene, diallyl sulfide, diallyl disulfide and diallyl trisulfide. The garlic oil is used in food applications as flavor, but is easy to be evaporated in short period. In food field, edible and natural materials are necessary, but due to the requirement of low cost, there is not much research working on it. The garlic oil used in thesis is from market commodity to keep the possibility of garlic oil's utilization.

1.5.7 Holy basil oil (HBO)

The genus *Ocimum* is represented by more than 150 species that widely grown and distributed throughout tropical and temperate regions, which is named as basil. From plants grown with same condition, Thai holy basil consists of linalool with other components being camphor and humulene which showed sweet-subtle aroma to oil. In (Thai) holy basil, estragole, geraniol and nerol are the major components contributing to the flavor. The holy basil in thesis is common fragrance in market which is utilized in fast food fields.

2. Methods

2.1 Properties of rice granule in thermo-responsive swelling and shrinking

A hundred milligrams of rice granules (stem from *Oryza sativa* grains, Branded Lotus, Thai Flour Industry, Bangkok, Thailand) were distributed in 40 mL water in closed round-bottomed flask to be heated at 80 °C for 30 mins. First portion of granules were subjected to confocal microscopic analysis (Confocal Laser Scanning Microscope, Eclipse, Ti series microscope, Nikon, Japan (and scanning electron microscopic (SEM, JEOL JSM-6480LV) immediately, the residual granules were kept at 4 °C for 24 h in refrigerator and sent to microscopy and SEM analysis. Analogous experiment was conducted by rising temperature to 100 °C.

2.2 Stability

To explore the stability of rice granule, multiple treatments on rice granules were carried out, including weak acid, alkaline treatments and various enzymes actions such as α -amylase, trypsin, lipase and papain to simulate environment of starch processing in human digest system.

Weak alkaline treatment: Rice granules was dispersed into 0.05 M aqueous NaOH solution by proportion at 1g/5ml, mixture was stirred continuously for 6 h at room temperature around 33 °C. Granules treated were subjected to SEM analysis directly.

Weak acid treatment: Acid is mostly used in starch industry to isolate starch granules from kernels to move proteins connect granules into a whole grain. Mixture with same proportion of rice granule and 0.05 M aqueous HCl solution at 1g/5ml was stirred for 6 h at room temperature. Samples were sent to SEM immediately.

α -Amylase treatment: Mixture of rice granules and 0.01 M phosphate buffer with PH 7.4 by proportion at 1g/5ml was added with α -Amylase (240000 units of α -amylase enzyme from *Bacillus subtilis*, Sigma-Aldrich, Singapore) and stirred at around 33 °C, the treated granules were collected and sampled at 1 and 3 h and then observed by SEM. Furthermore, to observe the reaction by fresh saliva with proportion of saliva, rice granule and water at 80 μ L/10mg/1ml, and gentle shaking at 37 °C. Similar experiment was executed using 0.01 M phosphate buffer with PH 7.4 instead of water.

Lipase treatment: Lipase enzyme solution was prepared by dissolve lipase (5 mg, 2000 units, from porcine pancreas, Type III, lyophilized cake, Sigma-Aldrich) in 0.05 M sodium carbonate solution (7 mL), and then incubated with rice granules loaded with vancomycin to be shaken at 37 °C. Samples were collected at 6 and 8 h to SEM analysis.

Trypsin treatment: Trypsin enzyme solution was prepared by dissolve trypsin (5 mg, 65000 units, from porcine pancreas, Type IX-S, lyophilized powder, Sigma-Aldrich) in 1 mM HCl solution (50 mL), and rice granules loaded with vancomycin (1g) was added in to keep stirring for 6 h. Finally samples were subjected to SEM analysis.

Papain treatment: Rice granules encapsulated with vancomycin (1g) was mixed with 0.01 M phosphate buffer saline (50ml, PH=7.4) to achieve the suspension, and then papain (1000 mg, 10000 units, from papaya latex, lyophilized powder, Sigma-Aldrich, Singapore) was mixed in to stir for 6 h at room temperature, and sample was

subjected to SEM analysis. Another multiple treatment on rice granule was carried out by rice granule, papain and water at proportion of 2.5mg/2.5mg/1ml containing 50 mg rice granules, and stirred at room temperature for 6 h. Subsequently 2 ml α -amylase suspension (α -amylase : water at 1mg/1ml) was added into and stirred at 37 °C for 1 h, and sample was collected to SEM.

2.3 Vancomycin encapsulation

Fifty milligrams of rice granules were mixed with 20 ml aqueous solution of vancomycin (Vancocin-S, Siam Pharmaceutical Co. Ltd., Thailand; 1 mg vancomycin in 1 ml). This mixture was stirred at 80 °C for 3 h. The granules were separated from the supernatant by centrifugation, washed with water and then kept at 4 °C. Similar experiments were also carried out with different initial concentrations of vancomycin to observe the concentration-related effect to loading efficiency and capacity: 1,000 ppm, 3,000 ppm, 5,000 ppm, 10,000 ppm and 20,000 ppm, respectively.

Quantized analysis and calculation of the amount of un-encapsulated vancomycin in the supernatant was measured step by step: First, centrifugal filters (Amicon® Ultra 0.5mL Filters, molecular weight cut off at 10,000) acted on the final mixture (mixture of granules achieved encapsulation and drug solution after heated at 80 °C for 3 h) to separate granules loaded with vancomycin from supernatant; second, quantifies the number of drug in dissociated supernatant after centrifugation by using UV-visible spectrophotometry (Optizen Pop Serise, Korea) taking purpose of the calibration curve contributed from vancomycin standard liquids prepared in DI water. So the encapsulated vancomycin content, encapsulation efficiency (EE%) and loading capacity (Loading%) can be performed by the equations below:

$$EE\% = \frac{\text{weight of drug encapsulated}}{\text{weight of total drug}} \times 100\%$$

$$\text{Loading}\% = \frac{\text{weight of drug encapsulated}}{\text{weight of drug carrier} + \text{weight of drug encapsulated}} \times 100\%$$

Granules loaded with vancomycin at 80% loading capacity were incubated by papain digestion for 3 h using the same proportional protocol as the rice granules. After

digestion, the vancomycin released from digested granules was analyzed by UV-Visible.

2.4 Encapsulation of curcumin

400 mg curcumin was dissolved into 1000ml 25% ethanol solution. For encapsulation process, 50 mg rice granules were mixed with 40 ml 400ppm curcumin solution and heated in closed-bottom at 80 °C for 3 hours. After reaction, samples were washed by DI water, and sent to Confocal Microscope to observed by (561nm) laser.

2.5 Optimal microscopy

Nikon Confocal Laser Scanning Microscope (Eclipse, Ti series, Japan) analyzed the rice granules encapsulated with curcumin by using 561 nm laser.

2.6 Vancomycin release from granules

Release of vancomycin from granules was executed through the incubation of 25 mg of rice granules with 80% loading capacity (encapsulation process with initial concentration at 20000 ppm) soaked in 10 ml release medium (0.01 M phosphate buffered saline, 0.137 M of NaCl, PH = 7.4) enfolded by 12 kDa MW cutoff dialysis bag (Sigma-Aldrich) and dialyzed against 40 ml of same release medium (total volume of release medium 50 ml). This release system was done by utilization of jacketed container in which temperature of surrounding water in jacket was stable at 37 °C to simulate humanity environment. At every sampling point, 2 ml release medium outside the dialysis bag was extracted with replacement of same volume of fresh release medium to the system to hold the total volume consistent. Other release profiles with different loading capacity (5.6% and 31.58%, encapsulation process at 1000ppm and 5000ppm, respectively) were experimented by using same conditions. Collected aliquots were centrifuged with filtering cutoff at 10,000 and rotation speed at 10,000 rpm for 3 mins at room temperature, afterwards the supernatant was sent to do quantification test by UV-Visible, whereas peak of vancomycin is at 282 nm with aid of calibration curve same to the standard liquid that freshly prepared in same

medium. To confirm that there is no other factor or entity from granules obstructed the absorption of vancomycin at 282 nm, the blank used in UV absorption analysis was prepared uniformly to the samples, drug-free rice granules were tried to place instead of rice granules encapsulated with vancomycin. Although the system was controlled to keep sterilized, after 5 days the rice granule enfolded in dialysis bag still got contaminated.

2.7 Thermal Gravimetric Analyses

Thermal gravimetric analysis is technique in which mass of sample is monitored against time and temperature to get thermo-balance. So by observations to peak-change of samples,

Various granule samples were subjected to thermal gravimetric analyses (TGA, YRIS Diamond TG-DTA, High Temp 115 PerkinElmer instruments, S II Seiko instruments, Japan). Four samples were analyzed, including: 1) Original raw rice granules; 2) Vancomycin-loaded granules with loading capacity at 80%; 3) Vancomycin-loaded granules (with 80% drug loading content) that had been finished of release experiment for 72 h; 4) Pure-vancomycin, powder.

2.8 X-ray diffraction analysis

One way to probe into the chemical interactions within the rice granules is to examine their X-ray diffraction (XRD) pattern, which is showed by crystalline peak of samples. Five samples were selected to finish the XRD analysis: raw rice granules, rice granules treated by heat only (in water at 80°C for 3 h), vancomycin-loaded rice granules (vancomycin loading capacity at 80%), granules encapsulated with vancomycin (loading content at 80%) after release, which has 30% drug left and pure vancomycin, analyzed by XRD (Rikaku ultrima+ 2000 X-ray Diffraction, Japan). By comparing the peak change of different samples, structural information of different treatments could be observed, which will confirm the encapsulation is successful.

2.9 Tissue interaction

To confirm if the rice granules can be used as drug-carrier in tissue, the vancomycin-loaded granules were tested the inflammatory reaction in mice (animal care and use protocol followed the National Institutes of Health (NIH) USA (#85-23, revised 1985) was approved by the Institutional Animal Care and Use Committee of the Faculty of Medicine, Chulalongkorn University, Bangkok, Thailand. Male, C57BL/6 mice at 8-week-old were purchased from the National Laboratory Animal Center, Nakhornpathom, Thailand.). Subcutaneous injection of drug-loaded granules were performed under isoflurane under sterile condition. Mice hair above loose skin between shoulders was removed and cleaned by 70 % alcohol. Granules loaded vancomycin was dispersed in the PBS following concentration at 2.5mg/ml, and three groups were compared: group I with PBS injection only; The subcutaneous injection of rice granules was performed under isoflurane anesthesia under the sterile condition. In short, the hair above the loose skin between shoulders was removed and cleaned with 70% alcohol. Then 0.375 mg of rice granules at the concentration of 2.5 mg/mL dispersed in PBS or PBS control 150 μ l (n=5/ group, group I: injected with PBS only; group II: injected with rice granules in PBS; group III: injected with vancomycin-loaded at 80% loading% rice granules in PBS) was administered subcutaneously. The inflammatory skin reaction was processed by daily observation. Mice were sacrifice at 7 days post injection and the skin lesion was fixed in 10% formalin, paraffin-embedded and stained with periodic acid-Schiff reagent Hematoxylin and eosin stain (Sigma-Aldrich, St. Louis, MO, USA). The inflammatory cells were observed from the lesion.

2.10 Edible oils encapsulation

Each aromatic oil extract was encapsulated into rice granules using our previously reported procedure of vancomycin encapsulation. Briefly, the extracted oil (including GO, HBO, SBO, LO, BO, TTO and KLO, 5 ml) was dispersed into the mixture of rice granule (5 g) and water (45 ml) in the closed round-bottomed flask at 80 °C and stirred for 3 h. Then the mixture was kept at 4 °C for 24 h. On the second day, the water exhausted from the granules were disposed, leaving the final products as thick past.

2.11 Stability of oil (GO, HBO and LO) test

Here GO, HBO and LO were selected to finish the tests. Stability of the original aroma oils and the encapsulated oils were compared. Fresh extracted oils (GO, HBO and LO) were sent to GC-MS analysis under head-space method, named as fresh garlic oil, fresh holy basil oil, and fresh lemongrass oil, respectively. Each GO, HBO and LO extracted oils of 10 ml were kept in open bottom at room temperature for 6 days and sent to GC-MS analysis, named as Garlic oil 6 days, Holy basil oil 6 days, and Lemongrass oil 6 days, respectively. Samples of granules encapsulated with GO, HBO and LO at 90 g were kept in open bottoms at room temperature for 24 hours and 6 days, respectively, and sent to GC-MS analysis, which were named as “Rice granules encapsulated with garlic oil 24 hours”, “Rice granules encapsulated with garlic oil 6 days”, “Rice granules encapsulated with holy basil oil 24 hours”, “Rice granules encapsulated with holy basil oil 6 days”, “Rice granules encapsulated with lemongrass oil 24 hours”, and “Rice granules encapsulated with lemongrass oil 6 days”, respectively.

2.12 Gas Chromatography Mass Spectrometry (GC-MS) analysis

Agilent Technologies, 7890A GC system; Agilent Technologies, 7000 GC/MS Triple Quad. For both garlic oil-related and holy basil oil-related samples, starting temperature is: 50 °C, and final temperature is 250 °C, with temperature rate at 4 °C/min. Analysis was carried out at 8.09e-05 Torr.

Headspace aliquot samples preparation: all garlic oil-related samples (including Fresh garlic oil, Garlic oil 6 days, Rice granules encapsulated with garlic oil 24 hours, Rice granules encapsulated with garlic oil 6 days), holy basil oil-related samples (including Fresh holy basil oil, Holy basil oil 6 days, Rice granules encapsulated with holy basil oil 24 hours, Rice granules encapsulated with holy basil oil 6 days), and lemongrass oil-related samples (including Fresh lemongrass oil, Lemongrass oil 6 days, Rice Granules encapsulated with lemongrass oil 24 hours, Rice granules encapsulated with lemongrass oil 6 days) were kept in vials with 1 ml for oil-samples and 9 g for granule-samples. One milliliter of fresh, 24 hours, and 6 days oils (including garlic, holy basil, lemongrass oils) were added into vials(airtight with size at 20 ml,

dimension 75.5*22.5 mm) to leave around 58 mm height to sealed cap, whereas 9g of granules encapsulated with oils (garlic, holy basil and lemongrass oils) were put in vials that left with around 60 mm height to cap. All the vials were incubated in water-heater for 15 mins at 60 °C and vapor was extracted into syringe (Agilent) to finish the GC testing.

2.13 Applications in ready meals/fast foods

Here two oil-encapsulated granules: garlic-loaded and holy basil-loaded granules were applied into the recipes of Thai foods named “Fried garlic pork” and “Stir-fried holy basil chicken”. The same dishes made with fresh garlic and holy basil plants, garlic and holy basil oils, were also prepared with exactly same recipes. Dishes were prepared by professional chefs from Suan Dusit University, Bangkok, Thailand.

The rice granules encapsulated with garlic and holy basil oils were prepared 2 weeks before cooking to achieve the aromatic release processing.

For cooking site, different amounts of seasoning were put into the cuisine of Holy Basil Chicken and Garlic Pork differing from three condiments: , which were reheated before testing on the fifth day.

2.14 Sensory Taste evaluations

All the panels consisted of 15 professional tasters. The score of evaluation is between -5 to +5 representing worst to best. Taste of D0 samples were carried out immediately after cooking was finished. D5 samples were evaluated after heating the portion in a microwave oven at 2000 watt for 2 min, process was showed in Figure 13.



Figure 13. (1), Dishes preparation; (2), Dishes cooking; (3), Dishes separation; (4), Containing of dishes at 8°C for 4 days; (5), Evaluation preparation; (6), Testing;

After evaluations finished, analysis of variance was utilized to finish the illustrations of the tastes by different prescriptions. Evaluation scores from statistical analysis could directly show the effect of granules with encapsulated oils and oils only compared with fresh plant materials.

Variance by evaluation scores of dishes at different timing points was selected to be applied into the linear regression analysis with confidence interval (%) at 95 for both garlic and holy basil related samples.

Chapter III Experimental results

1. Thermo-responsive size change of the rice granules

By having an average size of around 4.5 ± 0.7 (average \pm SD) μm , the shape and appearance could be observed by SEM, shown in Figure 14. Because of the size of rice granules is dependent on the technology of milled and ground to starch, recently some brands of starch granules in market could achieve size of granules at 2-3 μm . Here rice granules without treatment showed polyhedron in shape, meanwhile edges and corners are sharply significant.

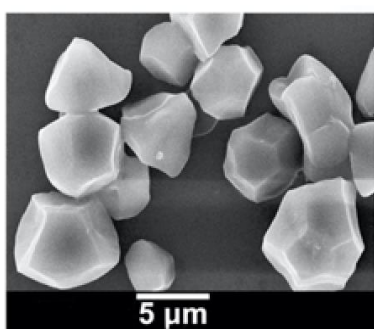


Figure 14. SEM of original rice granules without any treatment

After being heated aqueously at 80 °C and 100 °C for 30 mins, shape of granules kept same but average size changed to 8.5 ± 0.66 μm by both Confocal microscopic analysis and SEM images (Figure 15). Surfaces and corners of granules here were smoother compared with original granules. And when granules heated for same period at temperature lower than 70 °C, size of granule was not increased significantly. Granules with 30 mins heating at 80 °C were not destroyed, and when kept these granules in refrigerator at 4 °C for 24 hours, granules would shrink back to 4.4 ± 0.7 μm , shown in Figure 16. The shapes, edges and corners were much sharper and clearer than the one after heating. This indicates that water could penetrate into granules, and the swelling could support the whole granule expanding outward.

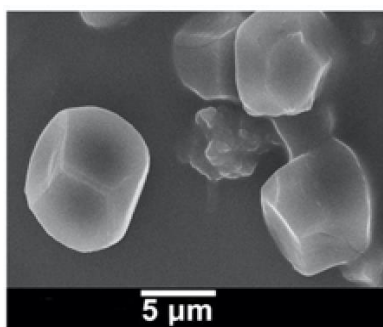


Figure 15. Granules treated by heating in water for 30 mins at 80 °C and 100 °C

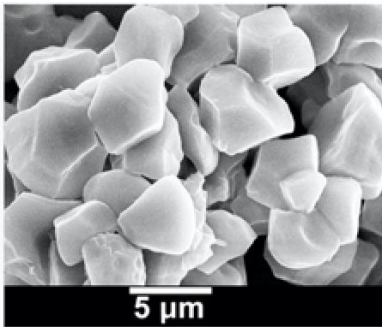


Figure 16. Granules heated at 80 °C for 30 mins and then kept in refrigerator at 4 °C for 24 h

These observations indicate that: (1). Size of granule can be expanded by heating in water and can be shrunk back to original when cooling at 4 °C; (2). The pentagonal shape of granule is preserved during the expansion. During the heat treatment, some of polymers especially amylose was leaked out from granules. The leak accounted for less than $29 \pm 6\%$ of polymer mass lost, which agrees well with the report before⁶⁰.

The shrinking and swelling ability of rice granules illustrates that there is no rigid membrane structure inside thermo-responsive granules. Situations of molecular packing inside granules are likely to be one of the main factors to determine morphologies. Among heating process, the thermal energy is used to destroy the strong interactions between polymers in granules, hence the polymer-water interactions could happen. Even though the polymer-water interaction provides less negative enthalpy than that from strong binding between polymer-polymer, the increase in entropy upon polymer swelling at higher temperature could help propelling the swell forward since the more negative Gibb free energy would be caused. Thus, the granule expands at high temperature together with water absorption into interior. After cooling, the entropy term becomes less significant at low temperature, so that the system accommodates to achieve more negative Gibb free energy by allowing the interactions between polymers to happen and getting larger heat release (larger than interactions between water and polymer). This process leads the shrinking of granules happening spontaneously at low temperature. And the water

inside heated-granules could be drained out from particles, which was observed when centrifuged heated granules kept at 4 °C.

Generally, it was noted that rice granule or starch can be considered as a thermo-responsive material. However, there are not many researches and reports on the stimuli-responsive rare material which is 100% nature. Other materials that have trigger functions such as light-responsive triblock copolymers, optically active and thermo-responsive star block copolymers, the redox-responsive micelles, which are specifically designed and assembled to get the stimuli-responsive mechanisms⁷²⁻⁷⁴.

2. Stability of rice starch

Based on the experimental observations and results, rice starch used in thesis is strikingly stable to various physical, chemical and biological treatments. Raw rice granules are from grinded kernels, and further hand-grinding could not destroy or change the size and shape. NaOH and HCl treatments to granules could not destroy granules, shown in Figure 17. Granules under these two chemical treatments still kept same shapes to original granules. So that rice granules are tolerant to base and acid at relatively low strength.

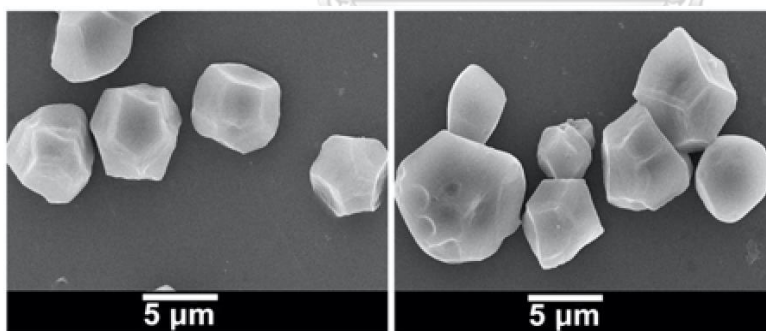


Figure 17. Left one is treated by NaOH(1g/5ml 0.05M NaOH solution, 6 hours); Right one is treated by HCl (1g/5ml 0.05M HCl solution, 6hours)

As widely accepted, amylose and amylopectin are major components in starch, but when incubated starch with α -amylase, an enzyme that used to digest starch from human saliva, did not produce breaking of granules, whereas structure of granules are well kept, and here only some changes on surface smoothness were observed, as

Figure 18 showed. This finding confirmed the hypothesis that the preservation of granular structure does not involve any membrane structure. This result illustrates that amount of accessible amylose and amylopectin at surface is quite limited.

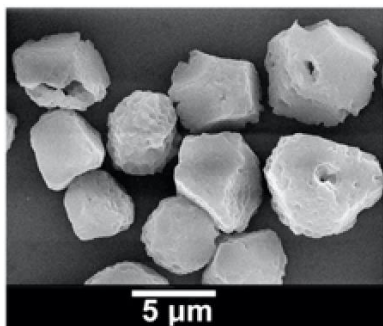


Figure 18. Rice granules treated by α -amylase (1260 U/1g, 37°C, 8 hours). Change on smoothness of surface observed by SEM

To simulate human stomach environment, trypsin treatment to granules was carried out. Nothing change on granules was surveyed after trypsin treatment, shown in Figure 19.

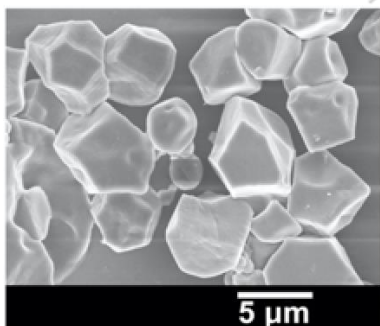


Figure 19. Rice granules treated by trypsin (65000U/1g, 6hours), nothing change was observed

Combined α -amylase and trypsin together, whatever which one first, could not produce any significant change to granules. And then lipase enzyme was used to treat granules resulting almost nothing different from original polyhedral granules with $4.5 \pm 0.68 \mu\text{m}$ in diameter, showed in Figure 20. Shape of granules were gotten a little less sharped. This implies lipid is not involved in granular shape and structure stabilization.

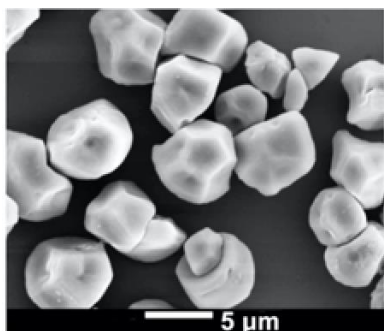


Figure 20. Granules treated by lipase at 37 °C for 6 hours (4000 U/ 1g)

And then, another enzyme papain, a protease with endopeptidase, amino-peptidase, and dipeptidyl peptidase activities, was tried to destroy granules, and observations showed that granules were lost their shapes, and collapse of granule was clearly happened, as Figure 21 illustrated.

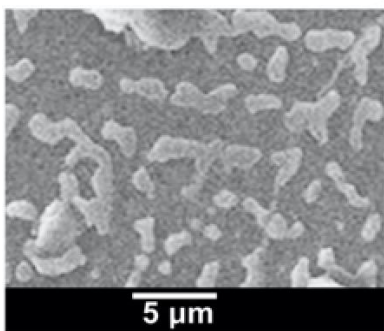


Figure 21. Granules incubated with papain at room temperature for 6 hours (50000 U/1g)

Afterwards, when α -amylase was used to act on papain-treated granules, complete destruction of granule was exhibited, shown in Figure 22.

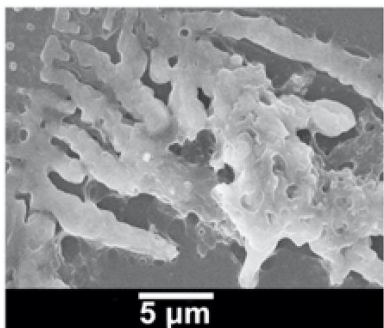


Figure 22. Granules incubated in papain solution (50000U/1g) at room temperature for 6 hours, followed with α -amylase solution at 80 °C for 1 hour (760U/1g)

Results above derive a hypothesis that granules contain amylose and amylopectin were packed with some proteins having stabilization function; absent of papain enzyme, amylose and amylopectin cannot be digested by α -amylase. The papain-sensitive proteins occupied small amount of arginine and lysine amino acid residues because they cannot be destroyed by trypsin. As discussed above, swelling of granules processes partial hydration. So the papain-sensitive proteins in granule would be responsible for granular shape stabilization, as well as function on un-swellable components of granules.

Results above contradict the assumption of digestion of rice granules in mouth and stomach where α -amylase and trypsin working on. And experimental results matched a fact that eating much rice could produce long-lasting energy release and good bulk in colon. So that rice granules in human digestive system are not fully digested and absorbed through mouth/stomach/small intestines but also being digested by microorganisms in colon. The resistance of granule to the complete digestion is contributing to the requirement on the bulk in colon to keep healthy environment for microorganisms⁶⁷. Ability of papain to destruct rice starch is worthy to mention, whereas traditional Thai cuisine of raw papaya (sauce of papain) with rice in northeastern Thailand was well known to support people with high energy for labor load. So that eating rice with papain could help releasing more carbohydrate from rice starch.

3. Encapsulation of vancomycin

Thermo-responsive rice granules were used to finish the encapsulation by incubating them in vancomycin solution at 80 °C for 3 hours. Here the. Amounts of drug molecules trapped into granules by detecting quantity of drug left in solution after separation out the granules by filtering centrifugation, which is named as indirect method. Another trial to perform the washing of drug-loaded granules by water and took into the calculation of amount of drug in washed solution as unloaded drug. These quantitative results clearly indicate that vancomycin can be loaded into granules with different loading contents depending on the initial concentration of vancomycin used in the experiment. Shape of vancomycin-loaded granules were observed by SEM, shown in Figure 23. It's clear that shape and morphology of loaded

granules were similar to heat-treated granules, and the ability of shrinking is weaker with size of $5.7 \pm 0.95 \mu\text{m}$ (after being placed at 4°C for 24 hours).

Here the encapsulation process can be summarized: during the swelling of granules in hot vancomycin solution, drug molecules together with water molecules penetrated into granules' interior and were trapped into granules. The encapsulation efficiency and loading capacity were increased with the increase of initial drug concentration, which was well agreed with the encapsulation mechanism proposed above that drug molecules occupy the interior of granules when heat-treated granule swelling while the solution gets into granules (Figure 23).

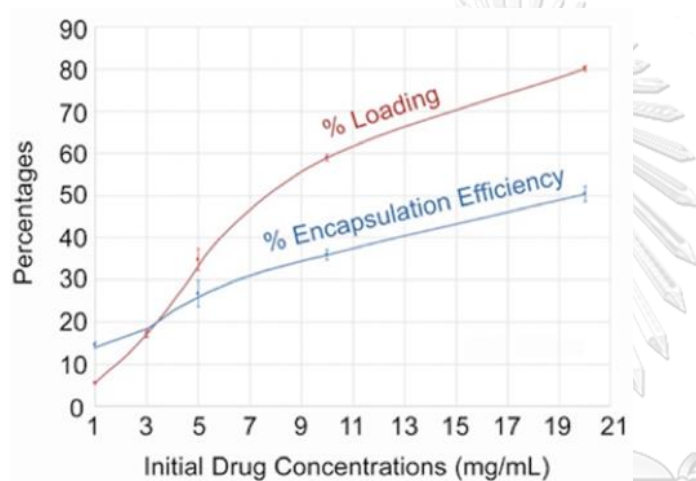


Figure 23. Efficiencies of the encapsulation process and loading contents of the obtained vancomycin-loaded granules, at various initial drug concentrations.

$$\%EE = [\text{wt. of drug in granules}/\text{wt. of drug in the original solution}] \times 100$$

$$\%Loading = [\text{wt. of drug in granules}/\text{wt. of the drug-loaded granules}] \times 100$$

Higher drug concentration means larger numbers of molecules at certain volume of solution. The limitation of swelling capacity restricts the amount of aqueous solution getting into granules. Hence, granules swollen in solution with high drug concentration should have higher number of drug molecules staying inside, compared with those swelled in solution with low drug concentration. After the penetration finished, vancomycin molecules may bind to polymer chains in granules through multiple hydrogen bonding, and are kept inside granules even after the granules were cooled at 4°C and water molecules expelled from granules, shown in Figure 24.

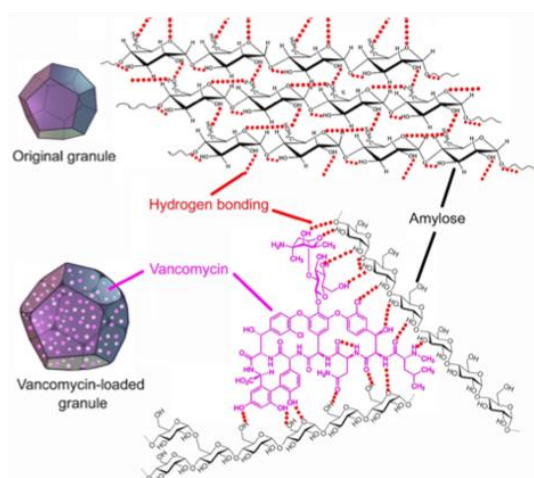


Figure 24. Model of vancomycin loading inside rice granule. Hydrogen bond interactions among amylose and amylopectin chains are disrupted in the presence of hydro-heating and vancomycin molecules which effectively form hydrogen bonding with the amylose and amylopectin chains.

4. Encapsulation of curcumin

By observation of Microscope with (500nm) laser, it was clearly showed that curcumin stayed both on surface and inside of granules, with granular size at around 7 μm . The fluorescence of curcumin is at green region, so that the 500nm laser source obviously triggered curcumin encapsulated in granules, which illustrated that hydrophobic substance could also encapsulated into granules, as Figure 25 showed.

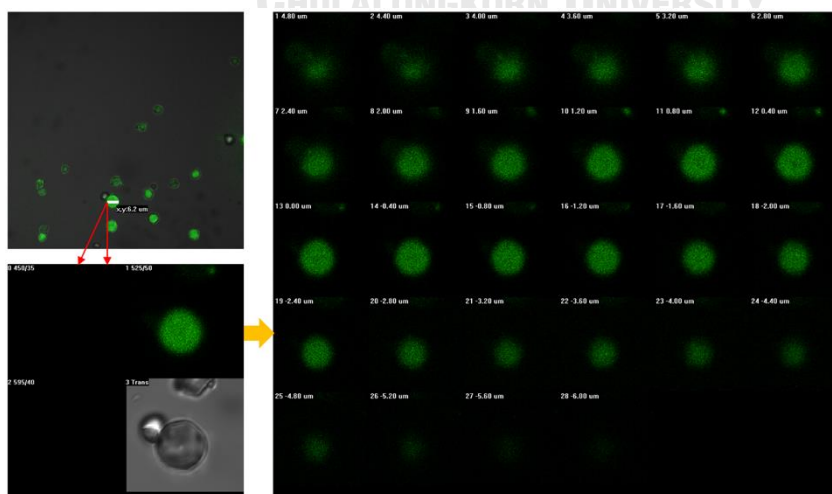


Figure 25. Confocal Microscope with 500 nm laser source to excite curcumin molecules

5. Release profile of vancomycin-loaded granules

Granules loaded with vancomycin at 80% loading content showed continuous release without burst. Steady sustained release of around 60% of drug in granules during 24 hours incubation in aqueous medium can be observed. And then release of around 10% of loaded drug was followed next day. And the cease of release afterwards was clearly shown afterwards (Figure 26). Experiments were carried out repeatedly along with replacement of release medium, where the stop happened as well to make sure the cease was not caused by high concentration of drug in release medium.

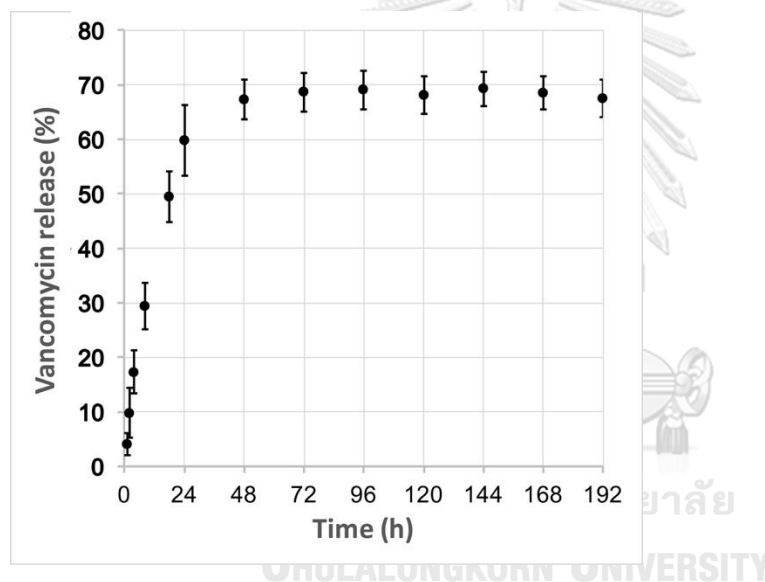


Figure 26. Accumulative release of vancomycin from vancomycin-loaded granules with 80% vancomycin loading content. The release was carried out by dispersing 25 mg of the vancomycin-loaded granules (80% vancomycin loading content) in 10 mL of 0.01 M phosphate buffered saline (0.137 M of NaCl, pH 7.4).

The result indicates that around 30% vancomycin in granule has strong interaction with components of granule that cannot be released out. Papain was added to digest vancomycin-loaded granules after 70% content release, but cannot observe the release of other remaining 30% drug. This result excludes the physical barrier as drug

sustainment factor, and confirms the molecular interaction between biopolymers (amylose and amylopectin) and vancomycin, which is responsible for the drug retention. Both papain and heating could not release the 30% drug left in granules. So there is around 30% of unreleased vancomycin because the strong interaction for granules loaded vancomycin at 80% loading content.

To make sure the 30% of unreleased vancomycin was not mis-interpreted from drug degradation, anthocyanin encapsulation was processed to get the direct observation by color. Granules loaded with anthocyanin gave similar release profile to that of vancomycin-loaded granules, but having purple color retained.

6. TGA results

The thermogram of raw rice granules shows relatively sharp endothermic peak at around 295-315 °C with maximum at 305 °C (as Figure 27 shows), which is consistent to the semi-crystalline structure. Alkaline-treated and heat-treated granules had similar thermograms to raw rice starch, as well as acid-treated granules. Data until now could conclude that aqueous heating (100 °C or less), and acid/alkaline treatments cannot disrupt the interactions among biopolymer chains within starch. Papain treated granules indicated the endothermic peak much broader with maximum of around 260-330 °C (maximum at 285 °C) compared with original granules, which was agreed with the SEM figures above that papain could effectively destroy the interactions between biopolymers. Thermogram of pure vancomycin displays a broad endothermic peak between 210-290 °C with maximum at 237 °C, corresponding to the non-crystal structure of vancomycin. Vancomycin-loaded granules with 80% loading capacity have much broader endothermic peak at 250-320 °C. Peak maxima of both raw granules at 305 °C and vancomycin at 237 °C disappeared, whereas new peak maximum at 265 and 302 °C, obviously illustrate the molecular interactions between vancomycin molecules and polymer constituents inside granules, meanwhile, disruption of original molecular interactions among polymer chains in the raw rice granules and achieve interactions with vancomycin molecules.

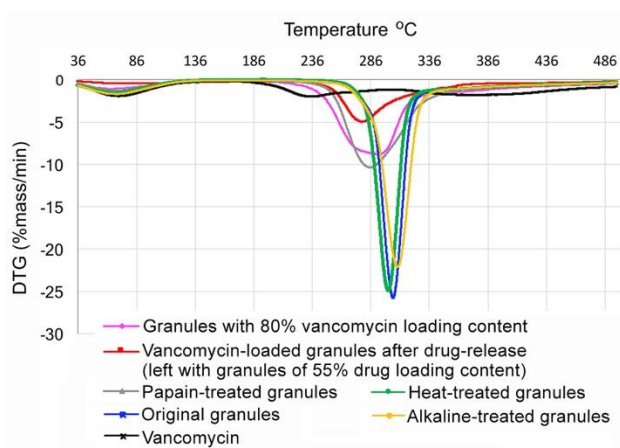


Figure 27. Thermal gravimetric analysis of granules with 80 % vancomycin loading content; vancomycin-loaded granules after incubating in release medium for 72 h (70% of the loaded vancomycin released out thus left with granules containing 55% vancomycin loading content); original granules; pure vancomycin; heat-treated granules and alkaline-treated granules.

These results vancomycin molecules and biopolymers in granules are in state of solid solution well distributed for vancomycin molecules in granules. IR analysis was carried out, but interaction between vancomycin and polymer constituents in granules cannot be witnessed from vancomycin-loaded granules, shown in Figure 28.

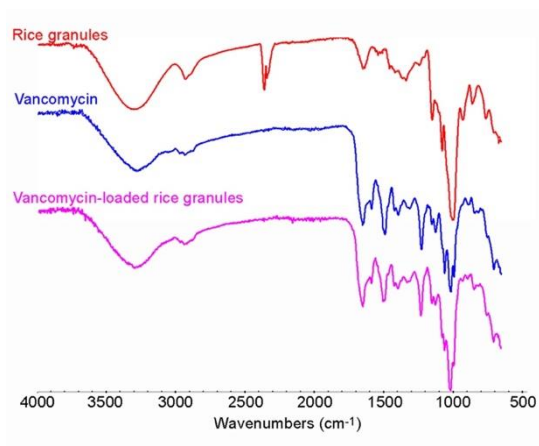


Figure 28. IR spectra of rice granules, vancomycin and vancomycin-loaded rice granules (with 80% drug loading content).

However, the IR spectrum of drug loaded granules confirmed the high loading content of drug molecules in granules as spectrum of drug-loaded granules resembles the spectrum of vancomycin. After incubating the vancomycin-loaded granules (80% drug loading content) in the release medium for 72 h, approximately 70% of the loaded drug should have been released out from the granules, the thermogram of the granules still shows roughly the broad peak at 260-300 °C, not much different in the peak shape from that of the vancomycin-loaded granules (before release), only lower in intensity. This also confirms the present of un-releasable vancomycin in the granules.

7. XRD results

XRD is most direct method to observe inter crystal structure of starch granules. The non-crystallinity was showed by XRD pattern of pure vancomycin, well corresponded to TGA peak, as Figure 29 shows. Raw rice granules with characters of semi-crystallinity displays three semi-sharp peaks at 17°, 18° and 23° of 2 θ . Pattern of heat-treated granules had similar peaks to raw granules but less sharp, which means the crystallinity of granules was minorly destroyed by heating.

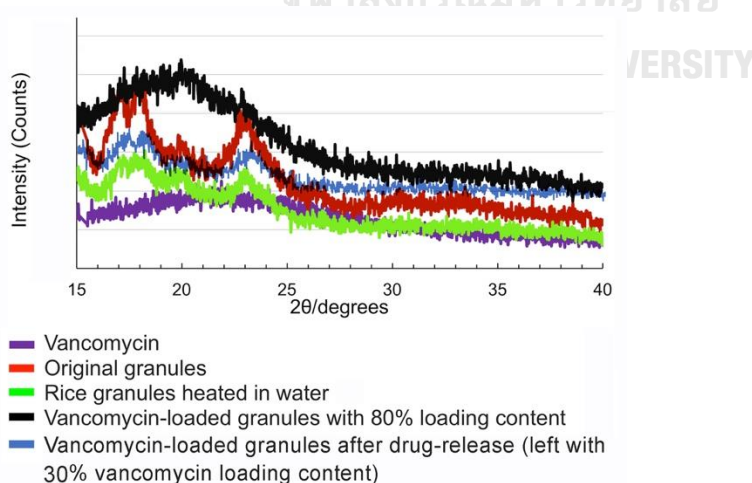


Figure 29. X-ray diffraction pattern of original granule, heat-treated rice granules, vancomycin-loaded granules with 80% loading content, the vancomycin-loaded

granules after the release experiment (left with 30% drug loading content), and vancomycin.

Vancomycin-loaded granules were significantly less crystalline than the unloaded granules, and the XRD pattern of the material showed a broad peak at 2θ of 20° . The disappearance of granule's crystallinity upon drug encapsulation illustrates the change in the molecular packing within the granules; vancomycin interference into the original ordered packing of the polymers plays the roles. Both the XRD and TGA results prove that, inside the granules, the direct interaction between vancomycin molecules and biopolymeric chains disrupts the molecular packing and crystallinity of the granules. XRD pattern of the drug-loaded granules after drug release was also carried out. As referred above, complete release can never be achieved, the granules possess approximately 30% drug loading after the release. Such granules show XRD pattern similar to the pattern of the unloaded granules. This indicates that molecular packing of the biopolymers was resumed after drug release.

8. Tissue interaction

As shown above that rice granules not only are indigestible by amylase in the mouth, trypsin in the stomach and lipase in the small intestine, here non-allergic of granules to tissue could be observed and also un-digestible by any enzymes under the skin. The reaction between granule injection and PBS injection (control) during the observation period were nothing different. In the histology at the 7-day post-injection, the granules were still intact with no significant inflammatory reaction. In addition, there was no eosinophil and basophil in the lesion, implying the non-allergic reaction of the granules in the mice. Due to the amounts of granules used in mice was limited, the non-allergic effect to the bio-system of skin part is understandable, based on the loading capacity of drug into granules can be very high, it is very possible for drug loaded granules to be applied into medical fields.

9. Edible oils encapsulation

By the encapsulation method described above, granules loaded with oils were achieved. During the encapsulation process, the mixture of garlic oil, water and rice granule was changed into dark yellow, whereas the ones with holy basil or lemongrass oil were changed into pale yellow by stirring with high speed. After 3 hours encapsulation, the whole mixture was found with sticky state without any movement. Following 24 hours storage in refrigerator at 4 °C, water exhausted from products was observed, and with none or very little oil floated upon which can be ignored.

Based on the equation of loading capacity, when implemented a protocol of 5 g rice granule encapsulated with 45 ml water and 5 ml oil, after keeping in refrigerator for 24 hours, around 10 ml water was exhausted. Then the loading capacity of oil trapped into granules is:

$$\text{Loading\%} = \frac{5}{5} \times 100\% = 100\%$$

Since the product was in the paste form, with water as the major ingredient, the amount of aroma oil in the paste was estimated to be

$$\% \text{ aroma oil in the paste} = \frac{5}{5+45} \times 100\% = 11\%$$

10. GCMS results

By GCMS analysis, major constituent of fresh garlic oil, garlic oil 6 days, and rice granules encapsulated with garlic oil for 6 days is monosulfide which was same to the literatures recently, shown in Figure 30, and the detailed information of key components in detected samples are shown in Table 5 and 6, all the MS are shown in Annex.

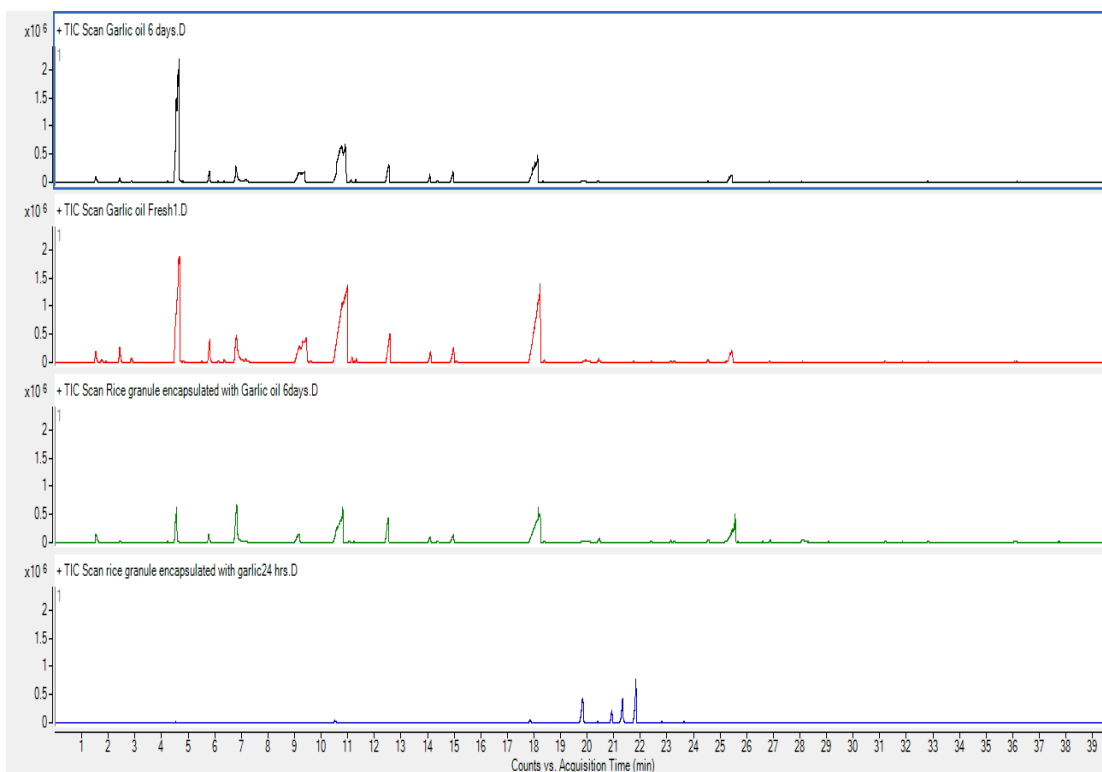


Figure 30. GCMS of garlic-related samples: fresh and 6 days oil; rice granules encapsulated with garlic oil for 24 hours and 6 days.

Table 5. Retention time of key components in samples (fresh garlic oil, garlic oil 6 days, and rice granules encapsulated with garlic oil for 6 days).

Compounds name	Retention Time (mins)
Propene (C ₃ H ₆)	1.541
Thiazoline (C ₂ H ₅ NS)	2.425
2,4-Dimethylthiazole (C ₅ H ₇ NS)	4.554
2-Ethyl-6-phenyl-5H-[1,3,4] thiadiazolo [3,2-a][1,3,5]triazine-5,7(6H)-dione (C ₁₂ H ₁₀ N ₄ O ₂ S)	5.772
4-Pyridinecarboxaldehyde (C ₆ H ₅ NO)	9.447
Thiodiacetonitrile (C ₄ H ₄ N ₂ S)	10.815
Tolycaine (C ₁₅ H ₂₂ N ₂ O ₃)	12.521

Propane-1,3-diamine. N, N'-bis(3-ethoxy-1-methyl-3-oxo-1-propenyl)- (C ₁₅ H ₂₆ N ₂ O ₄)	14.095
Propane-1,3-diamine. N, N'-bis(3-ethoxy-1-methyl-3-oxo-1-propenyl)- (C ₁₅ H ₂₆ N ₂ O ₄)	14.981
Thiodiacetonitrile (C ₄ H ₄ N ₂ S)	18.236
Acetic acid 2-isocyanoethyl ester (C ₅ H ₇ NO ₂ S)	25.368

Based on the results above, the existing of monosulfide components is well corresponded to the key aromatic components of volatile garlic oil. And these aromatic componets were well protected and can be released out, with differences only at intensity but not at retention times of peaks.

Table 6. Retention time of key components in sample of rice granules encapsulated with garlic oil for 24 hours.

Compounds name	Retention Time (mins)
2,6-Dimethylbenzothiazole (C ₉ H ₉ NS)	19.844
Bicyclo (2,2,1) heptane-2-acetonitrile, 5-cyano- (C ₁₀ H ₁₁ N ₂)	20.927
Benzeneacetonitrile, 3,4-dimethoxy (C ₁₀ H ₁₁ NO ₂)	21.343
1-Hexamine,N-(phenylmethylene) (C ₁₃ H ₁₉ N)	21.834

As shown in Figure 30 and Table 6, four new peaks were observed in sample of rice granules encapsulated with garlic oil 24 hours, which were not shown in other three samples. Observed from sample of rice granules encapsulated with garlic oil 6 days, the retention times of peaks were totally the same to fresh and 6 days garlic oil, but different intensities. The peaks in sample of rice granules encapsulated with garlic oil 24 hours disappeared after 5 days storage. This corresponds to the encapsulation capability of rice granule to be aromatic carrier.

Holy basil oil was also tried by GCMS, and the results are similar to granules-related experiments, shown in Figure 31. Retention time of fresh holy basil oil, holy basil oil 6 days and rice granules encapsulated with holy basil oil for 6 days are almost same, but different intensities, details are shown in Table 7. And in rice granules encapsulated with holy basil oil for 24 hours, four different new peaks could be observed compared with another three. All the details are shown in Table 7 and Table 8.

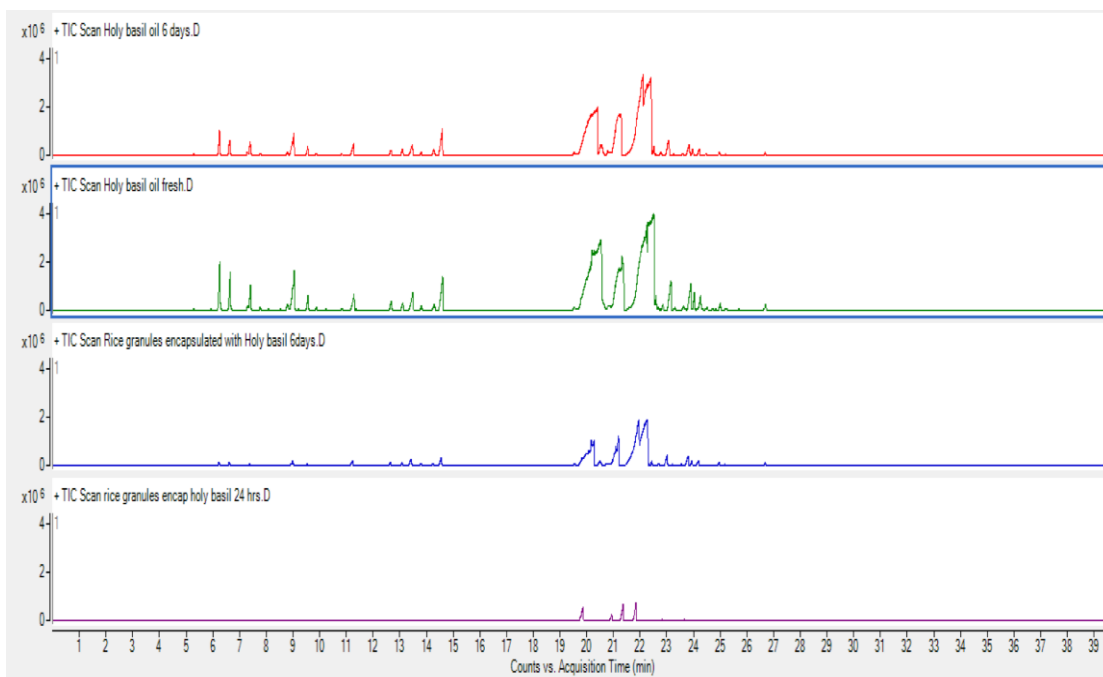


Figure 31. GCMS of holy basil-related samples: fresh and 6 days oil; rice granules encapsulated with garlic oil for 24 hours and 6 days.

Table 7. Retention time of peaks for fresh holy basil oil, holy basil oil 6 days, and rice granules encapsulated with holy basil oil 6 days.

Compounds name	Retention Time (mins)
Bicyclo[2.2.2]oct-7-en-2-one, 5-methylene- (C ₉ H ₁₀ O)	6.259
Pyridine,4(1,1-dimethylethyl)- (C ₉ H ₁₃ N)	6.648
3-Aminoacetophenone (C ₈ H ₉ NO)	7.411
9,10-Epoxy-4,8-ethanocyclohepta	9.566

(C ₁₁ H ₁₂ O ₄)	
Cis-8-Hydroxy-bicyclo (4,3,0) non-2-ene (C ₉ H ₁₄ O)	11.285
Cyclopentanecarbonitrile,2-imino- (C ₆ H ₈ N ₂)	12.676
4-Cyclooctene-1-carboxaldehyde (C ₉ H ₁₄ O)	13.116
3-Acetyl-1H-pyrroline (C ₆ H ₇ NO)	13.489
2-Pyridinamine 1-oxide (C ₅ H ₆ N ₂ O)	13.818
Benzeneacetamide (C ₈ H ₉ NO)	14.3
N-Benzhydrylidene-1-(2,4,6-trimethylphenyl) ethylamine N-oxide (C ₂₄ H ₂₅ NO)	14.607
4-Hydroxy-3-methoxyphenylacetonitrile (C ₉ H ₉ NO ₂)	20.551
Tryptamine (C ₁₀ H ₁₂ N ₂)	21.325
N-Nitrosornicotine (C ₉ H ₁₁ N ₃ O)	22.489
Dimethyl selenide (C ₂ H ₆ Se)	22.856
2-phenyl-2-(1,3-thiazol-2-ylsulfanyl) acetohydrazide (C ₁₁ H ₁₁ N ₃ OS ₂)	23.155
1-(4-Nitrobenzyl)-1H-imidazole (C ₁₀ H ₉ N ₃ O ₂)	23.634
4(1H)-Quinazolinone,2-methyl- (C ₉ H ₈ N ₂ O)	23.903
1-(2-Methoxyphenyl)2,5-dihydro-1H-pyrrole-2,5-dione (C ₁₁ H ₉ NO ₃)	24.268
2-Pyridinemethanol, α-4 pentenyl- (C ₁₁ H ₁₅ NO)	26.708

Table 8. Retention time of peaks for rice granules encapsulated with holy basil oil 24 hours.

Compounds name	Retention Time (mins)
Benzonitrile,3,4-dimethoxy- (C ₉ H ₉ NO ₂)	19.854
Tryptamine (C ₁₀ H ₁₂ N ₂)	20.933
5,6-Dimethoxyindole (C ₁₀ H ₁₁ NO ₂)	21.365
1-Hexanamine, N-(pherylmethylene)- (C ₁₃ H ₁₉ N)	21.842

Results of holy basil oil related samples showed that fresh holy basil oil, 6 days holy basil oil, and rice granules encapsulated with holy basil oil were having same peaks at different intensities, whereas rice granules encapsulated with holy basil oil 24 hours showing two peak same to other samples, and two new peaks. Functional groups with aromatic rings in most components encapsulated into rice granules were well preserved and released.

Lemongrass oil related samples were analyzed by GCMS as well, the results were similar to the garlic and holy basil experiments, showed in Figure 32. Peaks in fresh lemongrass oil, 6 days lemongrass oil and rice granules encapsulated with lemongrass oil 6 days were nearly same, and in rice granules encapsulated with lemongrass oil 24 hours lost 3 peaks from the other three. The components information in all samples were showed in Table 9 and 10. So the encapsulation on aromatic oils were achieved, and the release from granule was well implemented.

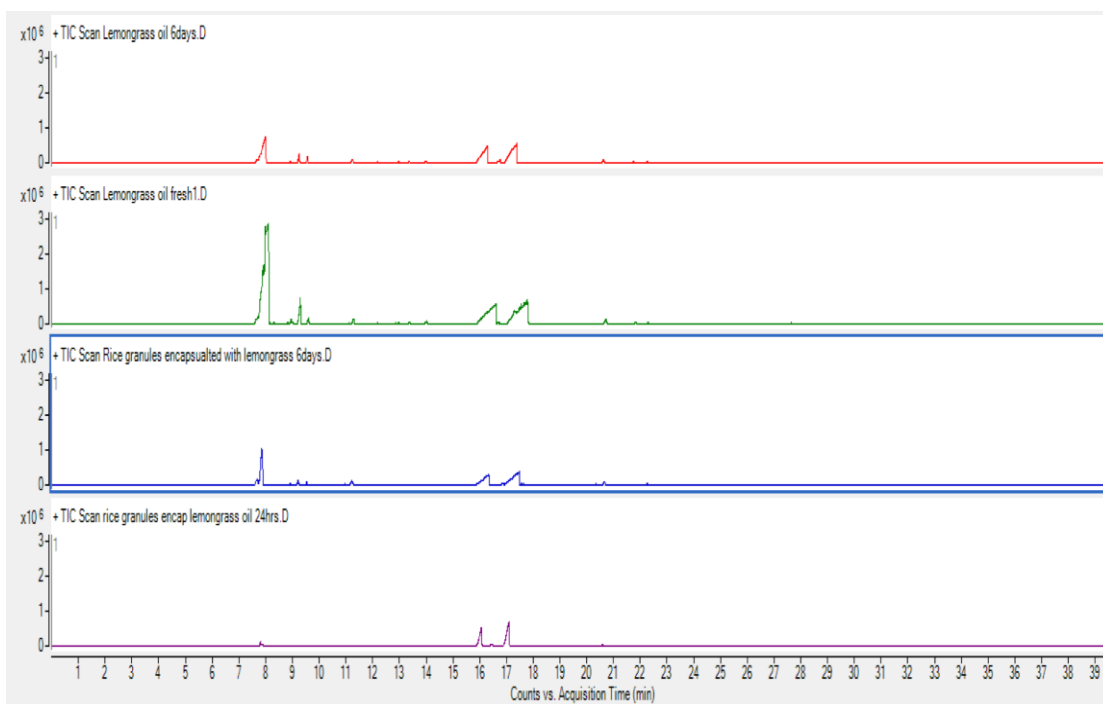


Figure 32. GCMS of lemongrass oil-related samples: fresh and 6 days oil; rice granules encapsulated with lemongrass oil for 24 hours and 6 days.

Table 9. Retention time of peaks for fresh lemongrass oil, lemongrass oil 6 days, and rice granules encapsulated with lemongrass oil 6 days.

Compounds name	Retention Time (mins)
(S)-2-benzylsuccinic acid (C ₁₁ H ₁₂ O ₄)	7.998
Bicyclo(3,2,1)oct-2-ene, 4-methylene-(C ₉ H ₁₂)	9.251
3-Cyclohexen-1-nitrile, 6-methyl-(C ₈ H ₁₁ N)	11.232
1-Methylcyclohexane-1-carbonitrile (C ₈ H ₁₃ N)	16.606
N-Ethyl-N-(2-propynyl) amine (C ₅ H ₉ N)	17.78
Limonene (C ₁₁ H ₁₂ O ₄)	20.73

Table 10. Retention time of peaks for rice granules encapsulated with lemongrass oil 24 hours.

Compounds name	Retention Time (mins)
----------------	-----------------------

(S)-2-benzylsuccinic acid (C ₁₁ H ₁₂ O ₄)	7.998
1-Methylcyclohexane-1-carbonitrile (C ₈ H ₁₃ N)	16.606
N-Ethyl-N-(2-propynyl) amine (C ₅ H ₉ N)	17.78
Limonene (C ₁₁ H ₁₂ O ₄)	20.73

Based on the results above, two peaks in fresh lemongrass oil, lemongrass oil 6 days, and rice granules encapsulated with lemongrass oil 6 days were not shown in rice granules encapsulated with lemongrass oil 24 hours, and other peaks were well preserved. Limonene (C₁₁H₁₂O₄) being the key aromatic consistently existed, which similar to the garlic and holy basil oil-related results.

Key volatile components from garlic oil-related, holy basil oil-related, and lemongrass oil-related samples are consistently same to the key aromatic compositions when kept for 6 days, but with different intensities. Rice granules to be carriers at 24 hours showed that the key aromatic components were more or less covered by granule matrix, and after a few days (6 days in experiment), the aromatic components could be reappeared, which is same to the original oils. So that rice granules to be oil-carriers are possible for food applications.

Observation by the results above, we could conclude that the functional groups of oils (including the ones with aromatic, anti-oxidation, anti-cancer functions) can be well preserved during long time storage. For instance, the monosulfide of garlic oil, aromatic ring of holy basil oil, and limonene in lemongrass oil to be the key aromatic compounds are all having good conservation by rice granule matrix, can be continuously released out. The consummate products processed transitional period at around 1 day, during this time, not all components are visible by GCMS, by the detection on samples at 6 days, all the components can be detected, and confirm the aromatic compounds in oils could be released to get the final “aromatic rice granules”.

11. AVONA statistical analysis

Result of statistical analysis was shown in Figure 33. Because of the smell and taste of Garlic pork dish are still intensively dependent on garlic, it's easy to explain that

score of garlic oil is highest for fresh cooking ones. After kept to the 5th day, dish made by granules encapsulated with garlic oil achieve best evaluation compared with another two, although the garlic oil in granules was only around 0.63 ml, whereas amount of garlic oil used was 1.5 ml. Thai Holy Basil dish highly depends on the smell of holy basil, that is more than garlic in garlic pork dish, so for fresh cooking ones dish utilized by holy basil oil got the best evaluation. And after 4 days storage, the one cooked by granules encapsulated with holy basil oil obtained highest score.

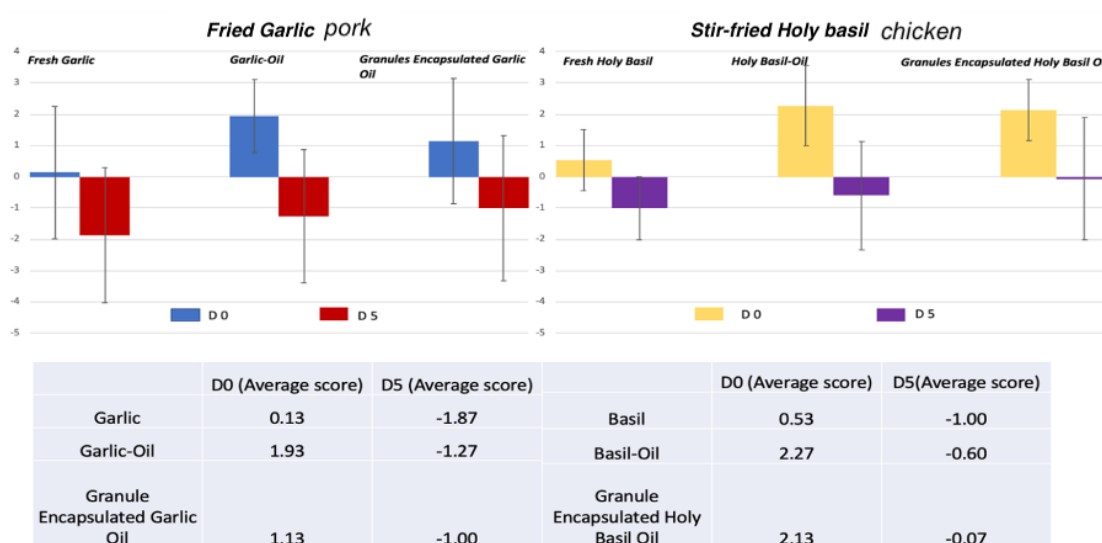


Figure 33. Evaluation results of Garlic pork and Thai Holy Basil chicken

Overall, granules encapsulated with oils got best evaluations than fresh plants and naked-oils after kept to the fifth day. So it's highly possible to apply these materials to fast foods.

Encapsulation into starch granules of hydrophilic substance is relatively easier compared to hydrophobic one, especially for the oil or oil-like materials. Shrinking of starch by heating at 80 °C and 4 °C refrigerator keeping could roughly confirm the success of oil encapsulation, due to the gel-like phenomenon without any layered showings between oil and water after heating, and water were exhausted and floated to the top of container after products kept in refrigerator at 4 °C for 24 hours, whereas product color were still close to oil. And by using of product in dishes cooking, the

smell of holy basil and garlic were continuously existing, so the oil was considered to stay inside granules, mechanism was shown in Figure 34.

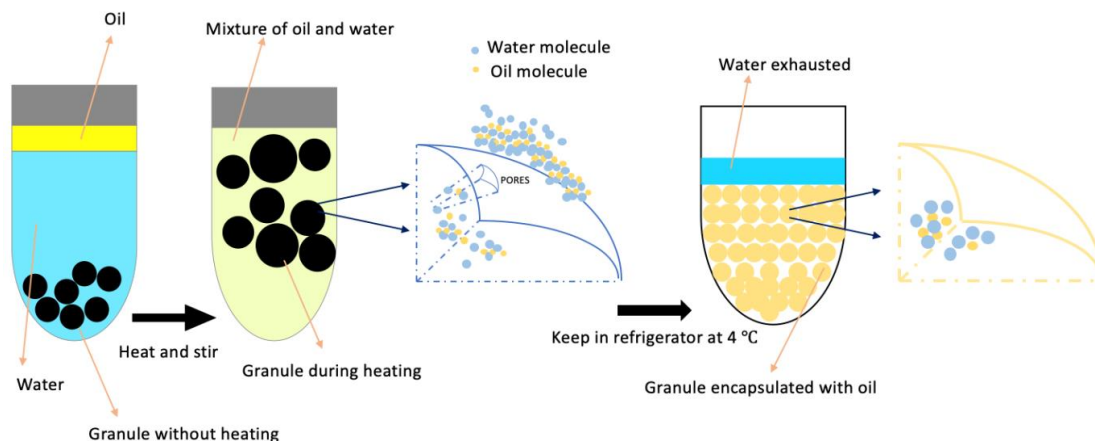


Figure 34. Mechanism illustration to the production of rice granule encapsulated with oil. During heating process, small pores or channels were generated by rice granule swelling, whereas water and oil molecules could get into granules. And by shrinking of granules in refrigerator at 4 °C, part of water in granules were exhausted, and left the granules with higher loading capacity.

When water and oil mixture penetrated into inside of granule at 80 °C, state of rice granule is at critical point of gelatinization. At this stage, hydrogen bonding between O-6 of amylose and OH-2 of amylopectin associates together, which is thermal stable. When the hydrogen bonding is formed, oil molecules can be locked inside granules, whereas key aroma components of oils can be kept under resistant of oxidization, light to contain the taste as fresh.

Chapter IV Discussion

1. Granules to be carriers

Dimensional structure of rice starch is generalized to be categorized into nano to micro levels ranging from 8.6 Å (glucose molecule) to hundreds nano meters (called growth ring). Granule of rice is relatively small compared with other starches, whereas size distribution is majorly in 2-9 µm, polyhedral in shape with smooth surfaces and density at 1.53 g/cm³. Commercial rice starch granule is utilized in this work due to its low cost, generality and practicality in medical and industrial applications.

The nano structure of inside granules consists with blocks having volume around $8 \times 10^4 \text{ nm}^3$, whereas the linkages between glucose units are through the upper end of anomeric carbon to form α-glucose. All the linkages and structural substance in starch have potentials to expand and absorb aqueous solutions. The swelling of rice granules heated in aqueous solution can be activated from 4.5µm to 8.5µm, which expanded around 6.74 times larger than original. So that the amount of loaded content is adjustable by varying the initial concentration of the solution. As Figure 23 shows, the loading efficiency and capacity are all increased with the initial concentration increasing. When starch is heated in water, granules experience water diffusion into, and lead to the swelling. Substance entrapped into granules as core material was connected to amylose and amylopectin by hydrogen bonds, and also locked inside by the amylose and amylopectin chains, as well as the hydrogen bonding between water molecules and starch.

As a glycopeptide antibiotic, vancomycin is preferred to cure patients of infections caused by methicillin-resistant staphylococcus aureus (referred as MRSA), which is actually used nearly 50 years to be penicillin alternative. It is considered to be an efficacious therapy empirically utilized to treat critical orthopedic infections with little toxic to osteoblasts and skeletal cells. Clinical tests and verifications observed vancomycin nephrotoxicity is showed in around 5-25% patients, which finally restrict the antibiotic dosage and duration of administration causing the incomplete bacterial eradication and resistance. Projects and researches aiming to solve this problem, delivery system of local antibiotics for the treatment of musculoskeletal infections are more and more attractive and necessary. Due to the hydrophilicity of vancomycin, it's

hard to control the release of mediums encapsulated or captured with vancomycin, so that the release system of vancomycin to achieve the lower incidence of toxicity must satisfy: tolerability, degradability, and high encapsulation efficiency (or loading capacity). The treatment to MRSA by vancomycin could be better when utilizing the rice granules encapsulated with drug, especially for the MRSA infection in digestive system.

Curcumin, also known as diferuloylmethane is a phenolic compound present in many kinds of medicinal plants, especially in *Curcuma longa* (turmeric). Curcumin has many pharmacological activities including antioxidant, anti-infection, anti-inflammation and anticancer. Because of curcumin's yellow color, it is convenient to be utilized in our work to observe whether the encapsulation is successful by naked eyes and optical microscopy. By the result, curcumin encapsulation was obviously successful.

Whatever the substance planned to be encapsulated into granules was hydrophilic or hydrophobic, it can be entrapped into granules when heated aqueously. In order to keep granules as visible carriers, what needs to be considered is only the heating temperature and period, to avoid the gelatinization happening.



2. Mathematical description of heating/encapsulation process

The encapsulation process in this work is by heating, due to the temperature is not higher than 80 °C, mathematical models are expressed to describe the amount and distribution of moisture, and volumetric expansion of the granules undergoing hygroscopic swelling. To simplify the conditions, all the theoretical estimations are followed by assumptions: starch matrix of rice granule is continuous, homogenous and isotropic; initial surface temperature of granule is equal to aqueous temperature; and the initial moisture content is homogenous. During our encapsulation process, rice granules would experience heating, water uptake and swelling, which all involve diffusion. In other words, encapsulation is pre-situation before gelatinization totally

happens, as Figure 35 showed. Water motion within rice granule is driven by chemical potential, hence the water molecules in aqueous environment would penetrate out layer of starch to inside. Encapsulation is partly thermal disordering of crystal structure in rice granules. Rate of granular swelling is influenced by the ratio of amylose and amylopectin, lipids, proteins, initial water content, and size of granules.

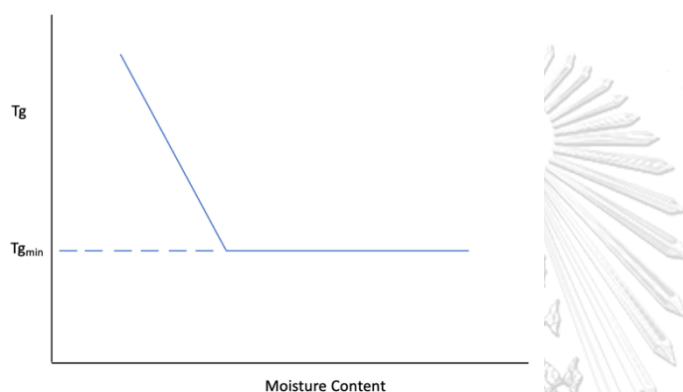


Figure 35. Gelatinization temperature versus moisture content. The temperature of gelatinization would increase with decreasing availability of water. T_g is gelatinization temperature, whereas $T_{g_{min}}$ is minimum gelatinization temperature (For rice, the maximum $T_{g_{min}}$ is not higher than 79 ± 10 °C generally, depends on the source).

1.1 Diffusion

During heating or encapsulation, mass and heat transfers are existing throughout all the process, so the model can be described based on Fick's law and Fourier's law:

$$\frac{\partial c_i}{\partial t} + \nabla \cdot (-D_i \nabla c_i) + u \cdot \nabla c_i = R_i \quad (1)$$

$$\rho C_p \frac{\partial T}{\partial t} + \rho C_p u \cdot \nabla T = \nabla \cdot (k \nabla T) + Q \quad (2)$$

where c_i , u and D_i are the water concentration (mol/m^3), velocity field (m/s) and water diffusion coefficient (m^2/s), respectively. R_i is mass generation (kg/m^3), C_p is specific

heat ($\text{J}/\text{kg}\cdot\text{K}$), ρ is the rice starch density (kg/m^3), k is the thermal conductivity ($\text{W}/\text{m}\cdot\text{K}$), T is temperature in Kelvins, and Q is heat production ($\text{W}\cdot\text{m}$).

1.2 Hygroscopic swelling

Rice starch processed by heating absorbs water and swell shown in Figure 36. So the hygroscopic effect (moisture induced effect, ε_{he}) is because of the swelling of starch molecules after absorbing water, which can be indicated by equation related with moisture content gradient (Δc) and hygroscopic expansion coefficient (β_h):

$$\varepsilon_{he} = \beta_h \Delta c \quad (3)$$

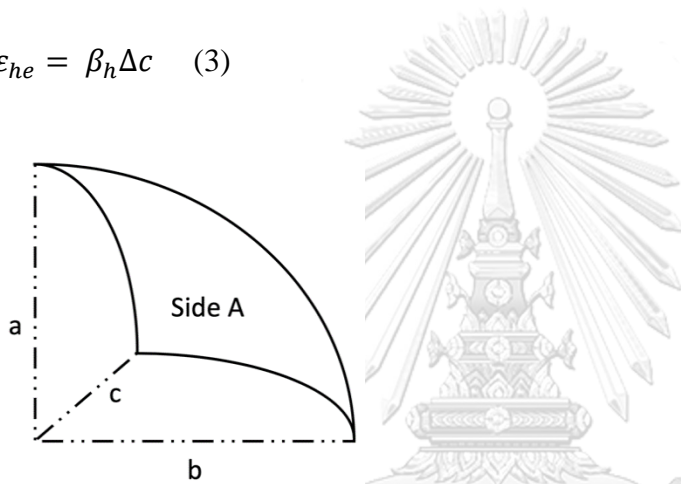


Figure 36. Schematic illustrating the granular geometry of boundary conditions for heat and mass transfer model. Starch assumed as spherical shape, $a=b=c=2000\text{-}3500$ nm, from spherical center to surface; side A is the interface of heat conduction, granular expansion and moisture acquirement by diffusion.

The boundary and initial conditions created for heat transfer in rice granule by processing equations below:

$$T = T_0, \text{ for } t = 0;$$

$$\frac{\partial T}{\partial t} = 0, \text{ for } r = 0; \quad (4)$$

$$\frac{\partial T}{\partial t} = k(T_w - T_0), \text{ for } t > 0;$$

where T_0 is temperature of rice granules not heated (in Kelvins), T_w is water temperature (in Kelvins), k is heat transfer coefficient ($\text{W}/\text{m}\cdot\text{K}$).

Conditions of mass transfer need to satisfy:

$c = c_0$, for $t = 0$;

$$\frac{\partial c_i}{\partial t} = 0, \text{ for } r = 0; \quad (5)$$

$$\frac{\partial c_i}{\partial t} = D(c_e - c_0), \text{ for } t > 0;$$

where t is encapsulation time (s), D is mass transfer coefficient (m/s), c_e and c_0 are equilibrium moisture content (kg/kg) and initial moisture content (kg/kg), respectively.

Because the diffusion coefficient of rice starch is dependent on temperature when treated by hydrothermal conditions, Arrhenius form relationship can be induced:

$$D_t = D_0 e^{-E_a/RT} \quad (6)$$

Here, R is universal rate constant, T is absolute temperature in Kelvins, E_a (activation energy) and D_0 are constant to be 4.148 J/mol and 1.203×10^{-5} , respectively.

Observations on the granular size change (volume increase of rice granule) combined with encapsulation time is showed in Figure 37, the volume increase is considered as amount of water uptake. In area I, the diffusion coefficient increases with temperature based on exponential law (equation 6). Therefore, the hydration rate turns into increasingly fast with the gradient of water concentration between surface and interior of rice granule was increased gradually. In stage II of preservation, the increasing rate of water absorption (volume expansion) continuous remains during the 180 mins heating.

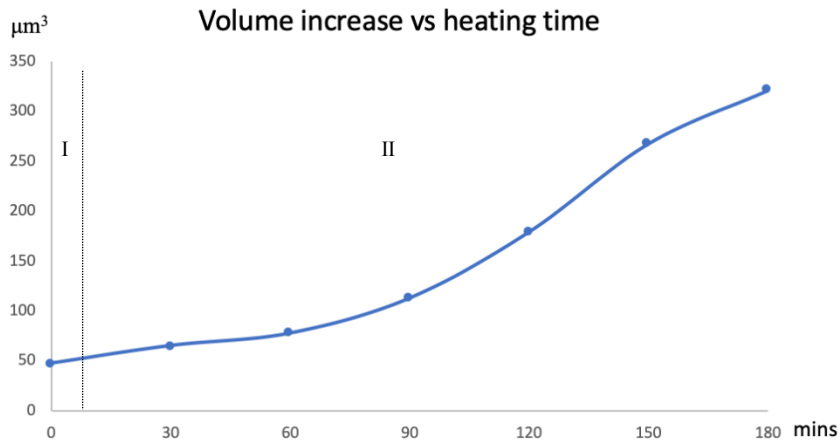


Figure 37. Volume changes of moisture content in rice granules during heating or encapsulation process at 80 °C. Area I is heating-up stage, which is shorter than 10 mins; area II is heating and encapsulation duration.

The volumetric change of rice granule at 80 °C is presented in Figure 38. Direction of water penetration and volumetric expansion are from out surface to interior, until water arrives at granular core, following the disintegration of granules if heating period is long enough.

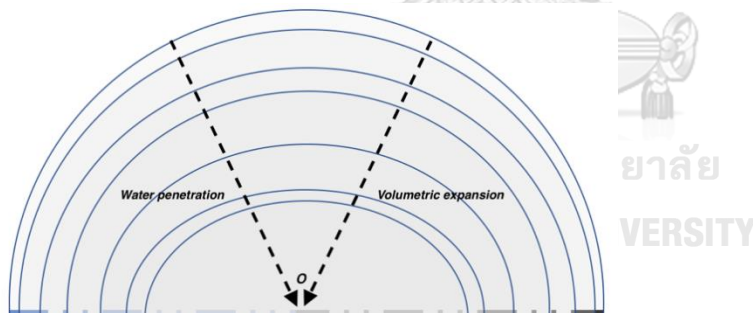


Figure 38. Simulation of moisture uptake in rice granules during the encapsulation treatment at 80 °C.

Encapsulation is a complicated process, which involves many situations like moisture uptake, starch gelatinization and swelling simultaneous. Water penetrated granule by observations on granular size change, from raw rice granule (diameter at 4.5 μm) to final product (diameter at 8.5 μm) step-by-step, whereas volume of granule would increase from 47.71 μm^3 to 321.65 μm^3 when granular shape is assumed as sphere, and heated at 80 °C for 3 hours.

1.3 Heating/Encapsulation

Here single rice granule is considered. Water or aqueous solution uptake can be expressed by derivation when granules swell by absorption of water. The basis of this calculation would be that at any point in granule water occupies a volume fraction ϕ , whereas $(1-\phi)$ is volume fraction of solid or starch. When water moves through granule it is assumed to displace the solid/starch on an equal volume basis. Taking u_s to be the actual velocity (m^3/m^2s) of solid at any point, u_w as the actual velocity of water and assuming rice starch has constant density, so conservation of solid and water at each point in granule can be expressed: (volumetric flux of water is ϕu_w .)

$$\frac{\partial \phi}{\partial t} + \nabla(\phi u_w) = 0 \quad (1)$$

$$\frac{\partial (1-\phi)}{\partial t} + \nabla[(1-\phi) u_s] = 0 \quad (2)$$

Combine the two equations to get:

$$\nabla [\phi u_w + (1-\phi) u_s] = 0 \quad (3)$$

$$2 \frac{\partial \phi}{\partial t} + \nabla [(u_w + u_s) \phi - u_s] = 0 \quad (4)$$

จุฬาลงกรณ์มหาวิทยาลัย
CHULALONGKORN UNIVERSITY

Assuming all velocities are in radial direction, whereas velocities are zero at center ($r=0$), so equation above can be integrated to produce:

$$\phi u_w + (1-\phi) u_s = 0 \quad (4)$$

For the flow in stationary porous matrix, equation can be generated by Darcy's law:

$$u = -k \nabla \Psi \quad (5)$$

where u is fluid velocity, Ψ is velocity potential, k is permeability of the porous medium. To simplify the derivation, consider the Ψ is function of ϕ only. During the swelling, aqueous flow passes through solid which is expanding until granule collapses. So fluid velocity can be replaced by $(u_w - u_s)$ to get:

$$u_w - u_s = -k\nabla\Psi \quad (6)$$

Combine equations (1), (4) and (6) together, equation (7) can be achieved:

$$\partial\phi/\partial t = \nabla[k\phi(1-\phi)(d\Psi/d\phi)\nabla\phi] \quad (7)$$

A new parameter called diffusivity as:

$$D(\phi) = k\phi(1-\phi)(d\Psi/d\phi) \quad (8)$$

it leads to nonlinear diffusion equation to describe water uptake:

$$\partial\phi/\partial t = \nabla(D(\phi)\nabla\phi) \quad (9)$$

Here, a spherical rice granule with radius R is considered, so the water volume fraction $\phi(r,t)$ satisfying:

$$r^2\partial\phi/\partial t = \frac{\partial}{\partial r}(r^2D(\phi)\frac{\partial\phi}{\partial r}) \quad (10)$$

When water is absorbed, surface of granular sphere has evolving surface with radius $R=R(t)$. To get equation for the change rate of $R(t)$ with time, the total mass inside the swelling sphere is gotten by integrating equation (10) over solid spherical volume as:

$$\int_0^{R(t)} \frac{\partial\phi}{\partial t} r^2 dr = \int_0^{R(t)} -\frac{\partial(1-\phi)}{\partial t} r^2 dr = \int_0^{R(t)} \frac{\partial}{\partial t} (r^2D(\phi)\frac{\partial\phi}{\partial r}) dr \quad (11)$$

Interchange time derivative and spatial integration to get:

$$[1-\phi(R(t),t)]R^2\frac{dR}{dt} = \frac{d}{dt} \left(\int_0^{R(t)} (1-\phi)r^2 dr \right) + R^2D(\phi(R(t),t))\frac{\partial}{\partial r}(R(t),t) \quad (12)$$

whereas $\frac{\partial \phi}{\partial r}(0, t) = 0$.

The left side on equation is proportional to the change rate of spherical volume. The first part on right side is proportional to the time rate of total solids volume change in rice granule. It accounts the solids loss and is nonzero when the dissolution of solids is considered. The second term on right side represents water flux through granular surface to contribute the increase in volume of granule. Due to there is no inhibiting outer pericarp in rice granules, the concentration at boundary is constant corresponding to saturation and equilibrium, and is expressed as:

$$\phi(R(t), t) = \phi_1 \quad (13)$$

Experiments indicates that ϕ_1 varies with temperature when higher than 60 °C. So that for a fixed temperature, ϕ_1 is constant. Based on equation (12), movement of outer boundary can be expressed as:

$$\frac{dR}{dt} = \left(\frac{D(\phi_1)}{1-\phi_1} \right) \frac{\partial \phi}{\partial r}(R(t), t) + \frac{1}{(1-\phi_1)R^2} \frac{d}{dt} \left(\int_0^{R(t)} (1-\phi) r^2 dr \right) \quad (14)$$

Or:

$$R^2 \frac{dR}{dt} = \left(\frac{D(\phi_1)}{1-\phi_1} \right) R^2 \frac{\partial \phi}{\partial r}(R(t), t) + \frac{1}{(1-\phi_1)} \frac{d}{dt} \left(\int_0^{R(t)} (1-\phi) r^2 dr \right) \quad (15)$$

Here condition of solid mass has to be assumed that the total mass of starch solid inside swelling granule is constant. Then the last term in equation (14) is zero, so it simplified evolution equation of R into:

$$\frac{dR}{dt} = \frac{D(\phi_1)}{1-\phi_1} \frac{\partial \phi}{\partial r}(R(t), t) \quad (16)$$

The change of radius is only dependent to water uptake, when water is absorbed, the whole granule swells, so dR/dt is proportional to velocity of starch at boundary, which is concluded as kinematic condition. As discussed above, water is uniformly distributed inside granule initially:

$$\phi(r,0) = \phi_0 \quad (17)$$

The moisture diffusivity is an intensively increasing function of moisture content. So there would be a critical state for gelatinization to happen, which is denoted as $s(t)$. As Figure 35 illustrates, at a certain temperature, gelatinization could happen under a certain moisture volume fraction, written as ϕ_g , so:

$$\phi(s(t),t) = \phi_g \quad (18)$$

After gelatinization totally happens, the situation of starch would be significantly different, especially for some parameters such as diffusivity, therefore diffusivity can be considered as discontinuous. Due to diffusivity before gelatinization is much smaller than gelatinization starts, so that $D(\phi)=0$ for $\phi < \phi_g$. And the ungelatinized region is same to initial moisture content $\phi(r,t) = \phi_0$ when $0 \leq r \leq s(t)$. Then the equation (17) of moisture volume fraction can be written as:

$$\phi(s^+,t) = \phi_g, \quad \phi(s^-,t) = \phi_0. \quad (19)$$

By integrating equation (10) from $r=s^-$ to $r=s^+$ to get:

$$\frac{d}{dt} \int_{s^-}^{s^+} \phi r^2 dr - (\phi_g - \phi_0) s^2 \frac{ds}{dt} = [s^2 D(\phi) \frac{\partial \phi}{\partial r}(s(t), t)]_{s^-}^{s^+} \quad (20)$$

Due to $D(\phi_0)=0$, and let $s(t)$ be inclined from s^+ and s^- to allow equation (20) being rearranged as:

$$\frac{ds}{dt} = -\frac{D(\phi_g)}{\phi_g - \phi_0} \frac{\partial \phi}{\partial r}(s(t), t) \quad (21)$$

Equation (20) could describe the evolution of starch boundary at critical state of gelatinization, which indicates the boundary between gelatinized and ungelatinized granules.

Gelatinization happens over a range of temperatures and moisture levels, where the curtail statement occurs. Subsequently the critical state moves to a manner dominated by moisture diffusion and balance, while any gelatinization kinetics are so fast that there is no rate-limited at this new manner which happened at a boundary called front. The outer radius, spatial variable, volume fraction, gelatinization front radius, diffusivity function and time are scaled according to:

$$\bar{R} = \frac{R}{l}, \quad \bar{r} = \frac{r}{l}, \quad \omega = \frac{\phi - \phi_0}{\phi_1 - \phi_0}, \quad \bar{s} = \frac{s}{l}, \quad D(\omega) = \frac{D(\phi)}{D(\phi_1)}, \quad \bar{t} = \frac{D(\phi_1)}{l^2} t \quad (22)$$

whereas l is initial radius of spherical granule. The balance of moisture volume fraction is function of temperature. In our encapsulation process held at a constant temperature, so that ϕ_1 is fixed. Therefore, equation (10) can be written as:

$$r^2 \frac{\partial \omega}{\partial t} = \frac{\partial}{\partial r} [r^2 D(\omega) \frac{\partial \omega}{\partial r}] \quad (23)$$

Clearly, this nonlinear diffusion equation contains initial conditions and boundary at:

$$\omega(r, 0) = 0, \quad \omega(R(t), t) = 1, \quad \omega(s(t), t) = \omega_g, \quad s(0) = 1, \quad R(0) = 1, \quad (24)$$

Here ω_g is scaled gelatinization moisture content:

$$\omega_g = \frac{\phi_g - \phi_0}{\phi_1 - \phi_0} \quad (25)$$

As Figure 35 illustrates, ϕ_g decreases with temperature increasing, whereas ϕ_1 may raise accompanied with the increase of temperature. Based on the combination of equation (15) and (21), could get:

$$\frac{dR}{dt} = \frac{\phi_1 - \phi_0}{1 - \phi_1} \frac{\partial \omega}{\partial r} (R(t), t) - \frac{1}{(1 - \phi_1)R^2} \frac{d}{dt} \left(\int_0^{R(t)} (1 - \phi) r^2 dr \right) \quad (26)$$

$$\frac{ds}{dt} = - \frac{D(\phi_g)}{D(\phi_1)} \left(\frac{\phi_1 - \phi_0}{\phi_g - \phi_0} \right) \frac{\partial \omega}{\partial r} (s(t), t) \quad (27)$$

For simplifying the cognition to the equations, 3 parameters are introduced: α , β , and γ .

$$\alpha = \frac{\phi_1 - \phi_0}{1 - \phi_1}, \beta = \frac{D(\phi_g)}{D(\phi_1)} \left(\frac{\phi_1 - \phi_0}{\phi_g - \phi_0} \right) = \frac{D(\omega_g)}{\omega_g}, \gamma(t) = - \frac{1}{(1 - \phi_1)R^2} \frac{d}{dt} \left[\int_0^{R(t)} (1 - \phi) r^2 dr \right] \quad (28)$$

Hence, equation (26) and (27) can be rewritten to:

$$\frac{dR}{dt} = \alpha \frac{\partial \omega}{\partial r} (R(t), t) - \gamma \quad (26')$$

$$\frac{ds}{dt} = -\beta \frac{\partial \omega}{\partial r} (s(t), t) \quad (27')$$

For encapsulation process, temperature is constant, so α and β are constants, and γ represents the dimensionless solid or starch dissolution rate.

Water uptake, gelatinization, granular swelling processed inside the spherical rice granules are described by equation (23). Here moisture content is considered to change largely, and water diffusivities at initial and final moisture contents are extremely different. Because the diffusivity is function of moisture content, water could penetrate granules by steep front. The outer hydro-heated region in granule is almost at diffusive steady state, so the moisture profile can be considered as pseudo-steady state, whereas only a little moisture transfer in core, and two zones are divided by gelatinization front $s(t)$. So $\partial \omega / \partial t \approx 0$ at outer region. Then equation (23) can be written as:

$$\frac{\partial}{\partial r} \left[r^2 D(\omega) \frac{\partial \omega}{\partial r} \right] = 0 \quad (29)$$

Due to it's in nonlinear diffusion profile, so the moisture distribution of hydro-content ω would satisfy the relation by introducing Kirchoff transformation (represented by F) to get:

$$F(\omega) = f\left(\frac{1}{r}\right) = \frac{M(t)}{r} + N(t) = \int_0^\omega D(x)dx \quad (30)$$

where M(t) and N(t) are functions of encapsulation or reaction time, without variable radius r; x is a variable for the convenience of calculation. By applying the boundary conditions in equation (28), the moisture profile ω could satisfy:

$$\frac{F(\omega) - F(\omega_g)}{F(1) - F(\omega_g)} = \frac{\frac{1}{s(t)} - \frac{1}{r}}{\frac{1}{s(t)} - \frac{1}{R(t)}} \quad (31)$$

to get relation of ω and r at time t when R and s are given.

Equations solved from (31) substituted into (26') and (27') to achieve:

$$\frac{dR}{dt} = \mathcal{H}_1 \frac{1}{R^2 \left(-\frac{1}{R} + \frac{1}{s}\right)} - \gamma \quad (32)$$

$$\frac{ds}{dt} = -\mathcal{H}_2 \frac{1}{s^2 \left(-\frac{1}{R} + \frac{1}{s}\right)} \quad (33)$$

and

$$\mathcal{H}_1 = \alpha [F(1) - F(\omega_g)] \quad (34)$$

$$\mathcal{H}_2 = [F(1) - F(\omega_g)] / \omega_g \quad (35)$$

Here, \mathcal{H}_1 , \mathcal{H}_2 and T are constants, whereas R(t) is the dissolution front and location of outer boundary. These results are effective when the gelatinization front almost arrives at center of granules.

By combining equations (34) and (35) through subscription in case of temperature is constant, new related equation can be gotten:

$$(R^3 - 1) = \frac{\mathcal{H}_1}{\mathcal{H}_2} (1 - s^3) \quad (36)$$

During encapsulation process, rice granules are considered without any starch dissolution because of the release of amylose and amylopectin is very little due to the

remaining of rice structure, then the starch dissolution rate γ is zero. So that equations (32) and (33) are combined to get the following expressions as:

$$s = \sqrt[3]{\frac{\mathcal{H}_2}{\mathcal{H}_1} \left(\frac{\mathcal{H}_1}{\mathcal{H}_2} + 1 - R^3 \right)} \quad (37)$$

Therefore, it can be deduced gelatinization time is the period of gelatinization front reaches at center of rice particle. So the radius of spherical granule at that time can be achieved by setting $s=0$. So equation (36) shows the maximum radius of swollen rice granule or saying as gelatinization radius before granular collapse:

$$R_g = \sqrt[3]{1 + \frac{\mathcal{H}_1}{\mathcal{H}_2}} \quad (38)$$

So when gelatinization is done, the volume expansion factor (referred as VEF) of single rice granule can be expressed by:

$$\text{VEF} = 1 + \frac{\mathcal{H}_1}{\mathcal{H}_2} = 1 + \alpha\omega_g \quad (39)$$

and by setting $s=0$, $R=R_g$ period to finish the swelling and start gelatinization can be gotten:

$$t_g = \frac{1}{2\mathcal{H}_1} \left[\left(1 + \frac{\mathcal{H}_1}{\mathcal{H}_2} \right) - \sqrt[3]{\left(1 + \frac{\mathcal{H}_1}{\mathcal{H}_2} \right)^2} \right] \quad (40)$$

Numerical calculation for fixed temperature at 80 °C.

Based on the observations of experiments, moisture volume fraction of gelatinization ϕ_g can be calculated by:

$$\phi_g = \frac{\text{final volume of granule} - \text{initial volume of granule}}{\text{final volume of granule}} = \frac{321.65 - 47.71}{321.65} = 0.85$$

where granular diameter changes from 4.5 to 8.5 μm after heated at 80 °C for 3 hours.

Diffusivity definition at fixed temperature can be introduced as:

$$D(\phi) = Ae^{c\phi},$$

whereas A and c are experimental constants, shown in Table 11⁷⁵.

Table 11. Parameter Values used for calculating water uptake.

Constants	Value
Density of rice granule	1.53 g/L
A	1.43×10^{-7}
c	5.22
ϕ_0	0.2
ϕ_1	0.8
ϕ_g	0.9
ω_g	0.9
α	3
\mathcal{H}_1	0.26
\mathcal{H}_2	0.1
VEF	3.7

For the case of no starch dissolution ($\gamma=0$), positions of $s(t)$ and $R(t)$ are functions of ϕ_g . If more water is needed to achieve gelatinization, the time required is also increased. This in turn shows an increase in amount of granular swelling.

Based on equation (40) and experimental basic data, period of gelatinization starting point is around 300 mins, which considered that the encapsulation time of our experiments is reasonably and theoretically correct for the applications.



จุฬาลงกรณ์มหาวิทยาลัย
CHULALONGKORN UNIVERSITY

Chapter V Conclusion

By the results above, the assembly of biopolymers into pentagonal granular structure of natural rice granules is stable against aqueous heating treatment (temperature lower than 80 °C for 3 hours, or 100 °C for 30 mins), diluted strong acids and bases, even though enzymes found in gut system, including amylase, lipase, and trypsin. But rice granules are not tolerant to papain enzyme, which can be effectively and totally digested by papain. By breaking the proteins embedded at granular surfaces, the whole structure of granules can be destroyed, which could conclude that proteins in granules stabilize the structure of granules, rather than the packing by amylose and amylopectin. Proteins in granules weakly influence the molecular weight distribution and crystalline structure, but play important role to stabilize the whole granular structure based on the results of papain treatment granules⁷⁶. Rice granules showed reversible thermo-responsive ability, whereas volume could possess size expanding from 48 μm^3 to 322 μm^3 and reduction when cooled. The thermo-responsibility of granule enhances the possibility of utilizing rice granules to be carrier. Both hydrophilic (vancomycin) and hydrophobic (curcumin, edible oils) substance were tried to achieve the encapsulation, and it's easy to observe the encapsulation of vancomycin and curcumin. The drug loading content of vancomycin can be up to 80%, which is better than some other encapsulation methods, and can be adjustable by varying the initial concentration. Except vancomycin, other hydrophilic substance like anthocyanin can achieve encapsulation as well. The color of granules encapsulated anthocyanin is partly resistant to light, which can be utilized into dye industry for food. Through XRD and TGA analysis, the interaction between vancomycin molecules and biopolymers can be confirmed. Vancomycin embedded inside rice granules can be released out in aqueous environment, with 60 % of the loaded drug being steadily released out in first day without burst release and 10 % of loaded drug being released in second day. The remaining 30 % vancomycin inside rice granules cannot be released out although papain enzyme was exerted. The stomach and colon-related diseases can be treated by granules contained corresponding drugs as long as adjusting the loading capacity to appropriate amount.

Encapsulation of edible oils was successful based on the experimental results, and rice granules could indeed protect and preserve the key aromatic components of oils. The smell and taste of aromatic granules are same to original oil, which is stronger than the fresh vegetables and plants. Compare the cooked foods prepared by fresh oil and granules encapsulated with oil, the taste of fresh ones gets higher evaluations than encapsulated ones, but after 4 days storage, the significant difference of evaluation was observed that dishes cooked by granule carriers are much better than oil ones. Rice granules as fragrance and aroma carriers are extremely attractive to the industries. All the materials used in the encapsulation of edible oils are all natural and eatable, so that rice granule is ideal for the utilization of food sector, especially for the fast food sold in supermarket.



REFERENCES



จุฬาลงกรณ์มหาวิทยาลัย
CHULALONGKORN UNIVERSITY

1. Whistler, R. L.; Bemiller, J. N.; Paschal, E. F.; Paschall., *Starch: Chemistry and Technology*. Academic Press: New York, **1984**.
2. Hizukuri, S.; Takeda, Y.; Maruta, N.; Juliano, B. O., Molecular structures of rice starch. *Carbohydr. Res.* **1989**, *189*, 227-235.
3. Juliano, B. O., Structure, chemistry, and function of rice grain and its fractions. *Cereal Foods World* **1992**, *37*, 772-779.
4. Wikman, J.; Blennow, A.; Bertoft, E., Effect of amylose deposition on potato tuber starch granule architecture and dynamics as studied by lintnerization. *Biopolymers* **2013**, *99*, 73-83.
5. French, D., Fine structure of starch and its relationship to the organization of starch granules. *J. Jpn. Soc. Starch Sci* **1972**, *19*, 8-25.
6. Popov, D. B., A.; Burghammer, M.; Chanzy, H.; Montesanti, N.; Putaux, J.-L.; Potocki-Véronèse, G.; Riekkel, C., Crystal structure of A-amylose: A revisit from synchrotron microdiffraction analysis of single crystals. *Macromolecules* **2009**, *42*, 1167-1174.
7. Imberty, A.; Pérez, S., A revisit to the three-dimensional structure of B-type starch. *Biopolymers* **1988**, *27*, 1205-1221.
8. Sanderson, J. S.; Daniels, R. D.; Donald, A. M.; Blennow, A.; Engelsen, S. B., Exploratory SAXS and HPAEC-PAD studies of starches from diverse plant genotypes. *Carbohydr. Polym.* **2006**, *64*, 433-443.
9. Putaux, J.-L.; Molina-Boisseau, S.; Momaour, T.; Dufresne, A., Platelet nanocrystals resulting from the disruption of waxy maize starch granules by acid hydrolysis. *Biomacromolecules* **2003**, *4*, 1198-1202.
10. Huber, K. C.; BeMiller, J. N., Visualization of channels and cavities of corn and sorghum starch granules. *Cereal Chem.* **1997**, *74*, 537-541.
11. Kim, H.-S.; Huber, K. C., Channels within soft wheat starch A- and B-type granules. *J. Cereal Sci.* **2008**, *48*, 159-172.
12. Buléon, A.; Bizot, H.; Delage, M. M.; Multon, J. L., Evolution of crystallinity and specific gravity of potato starch versus water ad- and desorption. *Starch/Stärke* **1982**, *34*, 361-366.
13. Tang, H.; Mitsunaga, T.; Kawamura, Y., Molecular arrangement in blocklets and starch granules architecture. *Carbohydr. Polym.* **2006**, *63*, 555-560.
14. Yoshimoto, Y.; Tashiro, J.; Takenouchi, T.; Takeda, Y., Molecular structure and some physicochemical properties of high-amylose barley starches. *Cereal Chemistry* **2000**, *77*, 279-285.
15. Bertoft., E., Understanding Starch Structure: Recent Progress. *Agronomy* **2017**, *56*, 1-29.
16. Takeda, Y.; Maruta, N.; Hizukuri, S., Examination of the structure of amylose by tritium labelling of the reducing terminal. *Carbohydr. Res.* **1992**, *227*, 113-120.
17. Hizukuri, S.; Takeda, Y.; Yasuda, M.; Suzuki, A., Multi-branched nature of amylose and the action of de-branching enzymes. *Carbohydr. Res.* **1981**, *94*, 205-213.
18. Takeda, Y.; Hizukuri, S.; Takeda, C.; Suzuki, A., Structures of branched molecules of amyloses of various origins, and molecular fractions of branched and unbranched molecules. *Carbohydr. Res.* **1987**, *165*, 139-145.
19. Gérard, C.; Barron, C.; Colonna, P.; Planchot, V., Amylose determination in genetically modified starches. *Carbohydr. Polym.* **2001**, *44*, 19-27.
20. Morrison, W. R.; Milligan, T. P.; Azudin, M. N., A relationship between the amylose and lipid contents of starches from diploid cereals. *J. Cereal Sci.* **1984**, *2*, 257-271.
21. Ren, S., Comparative analysis of some physicochemical properties of 19 kinds of native starches. *Starch/Stärke* **2017**, *68*, 1600367.
22. Kuakpetoon, D.; Wang, Y.-J., Internal structure and physicochemical properties of corn starches as revealed by chemical surface gelatinization. *Carbohydr. Res.* **2007**, *342*, 2253-2263.

23. Jane, J.-L.; Xu, A.; Radosavljevic, M.; Seib, P. A., Location of amylose in normal starch granules. I. Susceptibility of amylose and amylopectin to cross-linking reagents. *Cereal Chem.* **1992**, *69*, 405-409.
24. Myllärinen, P.; Autio, K.; Schulman, A. H.; Poutanen, K., Heat-induced changes of small and large barley starch granules. *J. Inst. Brew.* **1998**, *104*, 343-349.
25. Blazek, J.; Salman, H.; Rubio, A. L.; Gilbert, E.; Hanley, T.; Copeland, L., Structural characterization of wheat starch granules differing in amylose content and functional characteristics. *Carbohydr. Polym.* **2009**, *75*, 705-711.
26. Gidley, M. J., Molecular mechanisms underlying amylose aggregation and gelation. *Macromolecules* **1989**, *22*, 351-358.
27. French, A. D., Allowed and preferred shapes of amylose. *Bakers Digest* **1977**, *53*, 39-54.
28. Gernat, C.; Radosta, S.; Anger, H.; Damaschun, G., Crystalline parts of three different conformations detected in native and enzymatically degraded starches. *Starch/Stärke* **1993**, *45*, 309-314.
29. Vamadevan, V.; Hoover, R.; Bertoft, E.; Seetharaman, K., Hydrothermal treatment and iodine binding provide insights into the organization of glucan chains within the semi-crystalline lamellae of corn starch granules. *Biopolymers* **2014**, *101*, 871-885.
30. Morrison, W. R.; Laignelet, B., An improved colorimetric procedure for determining apparent and total amylose in cereal and other starches. *J. Cereal Sci.* **1983**, *1*, 9-20.
31. Putseys, J. A.; Lamberts, L.; Delcour, J. A., Amylose-inclusion complexes: Formation, identity and physico-chemical properties. *J. Cereal Sci.* **2010**, *51*, 238-247.
32. Yamashita, Y.; Monobe, K., Single Crystals of Amylose V Complexes .III. Crystals with 81 Helical Configuration. *J. Polym. Sci., Part A-2* **1971**, *9* (8), 1471-1481.
33. Debet, M. R.; Gidley, M. J., Three classes of starch granule swelling: Influence of surface proteins and lipids. *Carbohydr. Polym.* **2006**, *64*, 452-465.
34. Gilliard, T.; Bowler, P., Morphology and composition of starch. *Critical Reports Appl. Chem.* **1987**, *13*, 55-78.
35. Annor, G. A.; Marcone, M.; Bertoft, E.; Seetharaman, K., Unit and internal chain profile of millet amylopectin. *Cereal Chem.* **2014**, *91*, 29-34.
36. Gayin, J.; Abdel-Aal, E.-S. M.; Manful, J.; Bertoft, E., Unit and internal chain profile of African rice (*Oryza glaberrima*) amylopectin. *Carbohydr. Polym.* **2016**, *137*, 466-472.
37. Goldstein, A.; Annor, G.; Blennow, A.; Bertoft, E., Effect of diurnal photosynthetic activity on the fine structure of amylopectin from normal and waxy barley starch. *Int. J. Biol. Macromol.* **2017**, *102*, 924-932.
38. Kalinga, D. N.; Waduge, R.; Liu, Q.; Yada, R. Y.; Bertoft, E.; Seetharaman, K., On the differences in granular architecture and starch structure between pericarp and endosperm wheat starches. *Starch/Stärke* **2013**, *65*, 791-800.
39. Kong, X.; Bertoft, E.; Bao, J.; Corke, H., Molecular structure of amylopectin from amaranth starch and its effect on physicochemical properties. *Int. J. Biol. Macromol.* **2008**, *43*, 377-382.
40. Zhu, F.; Bertoft, E.; Källman, A.; Myers, A. M.; Seetharaman, K., Molecular structure of starches from maize mutants deficient in starch synthase III. *J. Agric. Food Chem.* **2013**, *61*, 9899-9907.
41. Takeda, Y.; Takeda, C.; Mizukami, H.; Hanashiro, I., Structures of large, medium and small starch granules of barley grain. *Carbohydr. Polym.* **1999**, *38*, 109-114.
42. Laohaphatanaleart, K.; Piyachomkwan, K.; Sriroth, K.; Santisopasri, V.; Bertoft, E., A study of the internal structure in cassava and rice amylopectin. *Starch/Stärke* **2009**, *61*, 557-569.
43. Matheson, N. K., The chemical structure of amylose and amylopectin fractions of starch from tobacco leaves during development and diurnally-nocturnally. *Carbohydr. Res.* **1996**, *282*, 247-262.

44. Meyer, K. H., The past and present of starch chemistry. . *Experientia* **1952**, 8, 405-444.
45. Walker, G. J. W., W.J.. The mechanism of carbohydrase action. 8. Structures of the muscle-phosphorylase limit dextrins of glycogen and amylopectin. *Biochem. J.* **1960**, 76, 264-268.
46. Bertoft, E., Partial characterisation of amylopectin alpha-dextrins. . *Carbohydr. Res.* **1989**, 189, 181-193.
47. Gidley, M. J.; Bulpin, P. V., Crystallisation of malto-oligosaccharides as models of the crystalline forms of starch: Minimum chain-length requirement for the formation of double helices. *Carbohydr. Res.* **1987**, 161, 291-300.
48. Bertoft, E.; Koch, K.; Åman, P., Building block organisation of clusters in amylopectin of different structural types. *Int. J. Biol. Macromol.* **2012**, 50, 1212-1223.
49. Kong, X.; Corke, H.; Bertoft, E., Fine structure characterization of amylopectins from grain amaranth starch. *Carbohydr. Res.* **2009**, 344, 1701-1708.
50. Bertoft, E., Composition of building blocks in clusters from potato amylopectin. *Carbohydr. Polym.* **2007**, 70, 123-136.
51. Laohaphatanaleart, K.; Piyachomkwan, K.; Sriroth, K.; Bertoft, E., The fine structure of cassava amylopectin. Part 1. Organization of clusters. *Int. J. Biol. Macromol.* **2010**, 47, 317-324.
52. Zhu, F.; Bertoft, E.; Seetharaman, K., Composition of clusters and building blocks in amylopectins of starch mutants deficient in starch synthase III. *J. Agric. Food Chem.* **2013**, 61, 12345-12355.
53. Bertoft, E.; Koch, K.; Åman, P., Structure of building blocks in amylopectins. *Carbohydr. Res.* **2012**, 361, 105-113.
54. Miles, M. J.; Morris, J.; V.; Ring, S. G., Gelation of amylose. *Carboh. Res.* **1985**, 135, 257-269.
55. Puteaux, J. L.; Buléon, A.; Chanzy, H., Network formation in dilute amylose and amylopectin studied by TEM. *Macromolecules* **2000**, 33, 6414-6422.
56. Tako, M.; Tamaki, Y.; Teruya, T.; Takeda, Y., The Principles of Starch Gelatinization and Retrogradation. *Food Nutr. Sci.* **2014**, 5, 280-291.
57. Moellering, R. C.; Jr., Vancomycin: A 50-Year Reassessment. *Clin. Infect. Dis.* **2006**, 42, S3-S4.
58. LaPlante, K. L.; Rybak, M. J., Impact of high-inoculum *Staphylococcus aureus* on the activities of nafcillin, vancomycin, linezolid, and daptomycin, alone and in combination with gentamicin, in an in vitro pharmacodynamic model. *Antimicrob. Agents Chemother.* **2004**, 48, 4665-4672.
59. Nitandai, Y.; Kikuchi, T.; Kakoi, K.; Hanamaki, S.; Fujisawa, I.; Aoki, K., Crystal Structures of the Complexes between Vancomycin and Cell-Wall Precursor Analogs. *J. Mol. Biol.* **2009**, 385 (5), 1422-1432.
60. Reynolds, P. E., Structure, biochemistry and mechanism of action of glycopeptide antibiotics. *Eur. J. Clin. Microbiol. Infect. Dis.* **1989**, 8 (11), 943-950.
61. Bassetti, M.; Merelli, M.; Temperoni, C.; Astilean, A., New antibiotics for bad bugs: where are we? *Ann. Clin. Microbiol. Antimicrob.* **2013**, 12, 1-15.
62. Y., C.; P., F.; G., M. C., Vancomycin-resistant enterococci. *Clin. Microbiol. Rev.* **2000**, 13, 686-707.
63. Güngör, S.; Delgado-Charro, B.; Ruiz-Perez, B.; Schubert, W.; Isom, P.; Moslemy, P.; A.Patane, M.; H.Guy, R., Trans-scleral iontophoretic delivery of low molecular weight therapeutics. *J. Control. Release* **2010**, 147 (2), 225-231.
64. Li, X.; Xu, J.; Filion, T. M.; Ayers, D. C.; Song, J., pHEMA-nHA Encapsulation and Delivery of Vancomycin and rhBMP-2 Enhances its Role as a Bone Graft Substitute. *Clin. Orthop. Relat. Res.* **2013**, 471, 2540-2547.

65. Elting, L. S.; Rubenstein, E. B.; Kurtin, D.; Rolston, K. V. I.; Fangtang, J. T.; Martin, C. G.; Raad, I. I.; Whimbey, E. E.; Manzullo, E.; Bodey, G. P., Mississippi mud in the 1990s: risks and outcomes of vancomycin-associated toxicity in general oncology practice. *Cancer* **1998**, *83*, 2597-2607.
66. Pai, M. P.; Mercier, R.-C.; Koster, S. A., Epidemiology of Vancomycin-Induced Neutropenia In Patients Receiving Home Intravenous Infusion Therapy. *Ann. Pharmacother* **2006**, *40*, 224-228.
67. Zakeri-Milani, P.; Loveymi, B. D.; Jelvehgari, M.; Valizadeh, H., The characteristics and improved intestinal permeability of vancomycin PLGA-nanoparticles as colloidal drug delivery system. *Colloids Surf., B* **2013**, *103*, 174-181.
68. Vinner, G. K.; Vladislavljević, G. T.; Clokie, M. R. J.; Malik, D. J., Microencapsulation of Clostridium difficile specific bacteriophages using microfluidic glass capillary devices for colon delivery using pH triggered release. *PLoS One* **2017**, *12* (10), e0186239.
69. Shahidi, F.; Han, X.-Q., Encapsulation of food ingredients. *Crit. Rev. Food Sci. Nutr.* **1993**, *33* (6), 501-547.
70. Bakry, A. M.; Abbas, S.; Ali, B.; Majeed, H.; Abouelwafa, M. Y.; Mousa, A.; Liang, L., Microencapsulation of Oils: A Comprehensive Review of Benefits, Techniques, and Applications. *Compr. Rev. Food Sci. Food Saf.* **2016**, *15* (143-182).
71. J, V.; C, D.; G, M.-R., Variables affecting lipid oxidation in dried microencapsulated oils. *Grasas Aceites* **2003**, *54*, 304-318.
72. Zhi-Peng, Y.; Na, L.; Li, Y.; Zhi-Qiang, J.; Zong-Quan, W., One Pot Synthesis, Stimuli Responsiveness, and White Light Emissions of Sequence Defined ABC Triblock Copolymers Containing Polythiophene, Polyyallene, and Poly(pheynl isocyanide) Blocks. *Macromolecules* **2017**, *50*, 3204-3214.
73. Wang, Q.; Ben-Fa, C.; Jia-Hong, C.; Na, L.; Zong-Quan, W., Facile Synthesis of Optically Active and Thermoresponsive Star Block Copolymers Carrying Helical Polyisocyanide Arms and Their Thermo-Triggered Chiral Resolution Ability. *ACS Macro Lett.* **2018**, *7*, 127-131.
74. Song-Qing, Z.; Guiju, H.; Xun-Hui, X.; Shu-Ming, K.; Na, L.; Zong-Quan, W., Synthesis of Redox-Responsive Core-Linked Micelles Carrying Optically Active Helical Poly(phenyl isocyanide) Arms and Their Applications in Drug Delivery. *ACS Macro Lett.* **2018**, *7*, 1073-1079.
75. Ramesh, M. N.; Srinivasa Rao P. N., Development and performance evaluation of a continuous rice cooker. *J Food Eng.* **1996**, *27*, 377-387.
76. HU, P.; FAN, X.; LIN, L.; WANG, J.; ZHANG, L.; WEI, C., Effect of surface proteins and lipids on molecular structure, thermal properties, and enzymatic hydrolysis of rice starch. *Food Sci. Technol.* **2017**, *38* (1), 84-90.

VITA

NAME LIU Xue

DATE OF BIRTH 24 Oct 1986

PLACE OF BIRTH YINGKOU City, LIAONING Province, CHINA

INSTITUTIONS ATTENDED Faculty of Graduate, Chulalongkorn University;

HOME ADDRESS MEISHUXINGCHENG residential,
HUANCHENGXIANG Street, GUANDU district,
KUNMING City, YUNNAN Province, CHINA.

PUBLICATION Natural Thermoresponsive Rice Granules as
Biocompatible Drug Carriers

AWARD RECEIVED -



จุฬาลงกรณ์มหาวิทยาลัย
CHULALONGKORN UNIVERSITY



จุฬาลงกรณ์มหาวิทยาลัย
CHULALONGKORN UNIVERSITY



จุฬาลงกรณ์มหาวิทยาลัย
CHULALONGKORN UNIVERSITY